

Cite this: *Dalton Trans.*, 2014, **43**, 5409–5426

## Accurate prediction of $^{195}\text{Pt}$ NMR chemical shifts for a series of Pt(II) and Pt(IV) antitumor agents by a non-relativistic DFT computational protocol†

Athanassios C. Tsipis\* and Ioannis N. Karapetsas

The GIAO-PBE0/SARC-ZORA(Pt)U6-31+G(d)(E) (E = main group element) computational protocol without including relativistic and spin-orbit effects is offered here for the accurate prediction of the  $^{195}\text{Pt}$  NMR chemical shifts of a series of *cis*-(amine)<sub>2</sub>PtX<sub>2</sub> (X = Cl, Br, I) anticancer agents (in total 42 complexes) and *cis*-diacetyl bis(amine)platinum(II) complexes (in total 12) in solutions employing the Polarizable Continuum Model (PCM) solvation model, thus contributing to the difficult task of computation of  $^{195}\text{Pt}$  NMR. Calculations of the torsional energy curves along the diabatic (unrelaxed) rotation around the Pt–N bond of the *cis*-(amine)<sub>2</sub>PtX<sub>2</sub> (X = Cl, Br, I) anticancer agents revealed the high sensitivity of the  $^{195}\text{Pt}$  NMR chemical shifts to conformational changes. The crucial effect of the conformational preferences on the electron density of the Pt central atom and consequently on the calculated  $\delta^{195}\text{Pt}$  chemical shifts was also corroborated by the excellent linear plots of  $\delta_{\text{calcd}}^{195}\text{Pt}$  chemical shifts vs. the natural atomic charge Q<sub>Pt</sub>. Furthermore, for the accurate prediction of the  $^{195}\text{Pt}$  NMR chemical shifts of the *cis*-bis(amine)Pt(II) anticancer agents bearing carboxylato- as the leaving ligands (in total 8) and a series of octahedral Pt(IV) antitumor agents (in total 20 complexes) the non-relativistic GIAO-PBE0/SARC-ZORA(Pt)U6-31+G(d)(E) computational protocol performs best in combination with the universal continuum solvation model based on solute electron density called SMD for aqueous solutions. Despite neglecting relativistic and spin orbit effects the agreement of the calculated  $\delta^{195}\text{Pt}$  chemical shifts with experimental values is surprising probably due to effective error compensation. Moreover, the observed solvent effects on the structural parameters of the complexes probably overcome the relativistic effects, and therefore the successful applicability of the non-relativistic GIAO-PBE0/SARC-ZORA(Pt)U6-31+G(d)(E) computational protocol in producing reliable  $\delta_{\text{calcd}}^{195}\text{Pt}$  chemical shifts could be understood. In a few cases (e.g. the dihydroxo Pt(IV) complexes) the higher deviations of the calculated from the experimental values of  $\delta^{195}\text{Pt}$  chemical shifts are probably due to the fact that the experimental assignments refer to a different composition of the complexes in solutions than that used in the calculations, and different hydrogen bonding and formation of dimeric species.

Received 21st December 2013,

Accepted 20th January 2014

DOI: 10.1039/c3dt53594k

[www.rsc.org/dalton](http://www.rsc.org/dalton)

## Introduction

$^{195}\text{Pt}$  NMR spectroscopy has been used successfully in platinum chemistry, owing to the importance of platinum compounds in cancer research (antitumor agents), in the area of biosensors and biomarkers and in catalysis. An overview of the  $^{195}\text{Pt}$  NMR spectroscopy describing some basic theoretical aspects and also the empirical approach used by researchers in the field has been published by Priqueler and co-workers in 2006.<sup>1</sup> Nowadays,  $\delta^{195}\text{Pt}$  chemical shifts have been reported for many platinum compounds and several trends have been noted, especially in the seminal review by Pregosin<sup>2</sup> and in the more recent reviews by Priqueler *et al.*,<sup>1</sup> by Osella and co-workers<sup>3</sup> and by Price *et al.*<sup>4</sup>  $^{195}\text{Pt}$  chemical shifts cover a wide range of values, about 15 000 ppm, from +8000 to -7000 ppm relative to  $\delta^{195}\text{Pt} = 0$  of the reference standard  $[\text{PtCl}_6]^{2-}$ .

Laboratory of Inorganic and General Chemistry, Department of Chemistry, University of Ioannina, 451 10 Ioannina, Greece. E-mail: attsipis@uoi.gr

† Electronic supplementary information (ESI) available: Complete author list for ref. 43. Structural and  $^{195}\text{Pt}$  NMR parameters of the  $[\text{PtCl}_6]^{2-}$  and  $[\text{PtCl}_4]^{2-}$  reference compounds calculated at various levels of theory (Table S1). The changes of the isotropic shielding tensor elements ( $\sigma^{\text{iso}}$ ) observed along the diabatic (unrelaxed) rotation around the Pt–N bond (Table S2). Selected structural parameters of the optimized geometries of the carboxylato- *cis*-bis(amine) Pt(II) anticancer agents (Table S3). Selected structural parameters for a series of diacetyl bis(amine) platinum(II) complexes (Table S4). Selected structural parameters (bond lengths in Å, bond angles in degrees) for octahedral Pt(IV) anticancer agents (Table S5). Cartesian coordinates and energies of antitumour agents (in Hartrees) (Table S6). See DOI: 10.1039/c3dt53594k

Despite the numerous experimental applications of  $^{195}\text{Pt}$  NMR spectroscopy, theoretical predictions of the  $^{195}\text{Pt}$  chemical shifts are rather limited. This is due to the difficulties intrinsic in the computational methods owing to the large number of electrons contributed by the heavy  $^{195}\text{Pt}$  atom, thus preventing routine calculations of  $^{195}\text{Pt}$  chemical shifts even in small-sized platinum complexes.<sup>5–8</sup> The first theoretical predictions of  $^{195}\text{Pt}$  chemical shifts were published by Pidcock *et al.*<sup>9</sup> and Dean and Green<sup>10</sup> in 1960, who applied Ramsey's equation for paramagnetic shielding to square planar Pt(II) complexes. The breakthrough in the calculation of the  $^{195}\text{Pt}$  NMR chemical shift can be related to the work of Malkin *et al.*<sup>11</sup> who employed DFT methods with a Kohn-Sham independent gauge for localized orbitals (IGLO). Later, Ziegler and co-workers calculated  $^{17}\text{O}$  NMR shielding tensors in transition metal oxides  $[\text{MO}_4]^{n-}$  and the  $^{195}\text{Pt}$  chemical shift for a series of Pt(II) complexes using a gauge including atomic orbitals (GIAO) and modern DFT methods. Despite the fact that reasonably fast computer codes for  $^{195}\text{Pt}$  NMR computations are now available,<sup>8,12</sup> to accurately predict  $^{195}\text{Pt}$  chemical shifts in solution remains a challenge, due to their sensitivity to the nature of the ligands, to the molecular structure of the complexes, and to the magnitude of solvent effects. Accordingly, the calculation of metal NMR parameters in solution requires elaborate computational approaches.<sup>7,12–14</sup>

Although there are well-established empirical rules to describe and interpret  $^{195}\text{Pt}$  chemical shifts,<sup>15</sup> methods rooted in DFT are particularly appealing due to their remarkable accuracy coupled with their efficiency in handling electron correlation.<sup>16,17</sup> In pioneering computations of  $^{195}\text{Pt}$  chemical shifts employing DFT methods, acceptable agreement with experiment was obtained only when a complex similar to the probe was used as a reference.<sup>18–22</sup> Gilbert and Ziegler<sup>18</sup> calculated the  $^{195}\text{Pt}$  chemical shifts for a series of Pt(II) complexes and showed that good agreement with experimental values is obtained when the contribution from spin-orbit relativistic effects to the chemical shielding tensor  $\sigma$  is taken into consideration employing (a) a zeroth order regular approximation (ZORA) method<sup>23</sup> and (b) a Pauli Hamiltonian method.<sup>24</sup> Sterzel and Autschbach<sup>13</sup> showed that for different platinum compounds  $^{195}\text{Pt}$  NMR remains a challenge for computational chemistry and that routine calculations cannot yet be performed easily with a well-defined computational model. More recently Truflandier and Autschbach<sup>25</sup> demonstrated that a combination of *ab initio* molecular dynamics (aiMD) and relativistic NMR methods based on DFT predict  $^{195}\text{Pt}$  chemical shifts for a set of platinum compounds in good agreement (within 10%) with experimental data.

Fowe and co-workers<sup>21</sup> employing the ZORA spin-orbit Hamiltonian, in conjunction with the gauge including orbital (GIAO) method based on DFT, calculated the  $^{195}\text{Pt}$  chemical shifts of  $[\text{PtCl}_x\text{Br}_{6-x}]^{2-}$  complexes. They found a strong dependence of the  $^{195}\text{Pt}$  chemical shifts on the bond lengths and solvation effects. It is well established that structural-, vibrational-, solvent-, and relativity-induced shielding effects are of primary

importance for the computation of NMR shielding tensors of heavy atoms.<sup>6–8,26</sup>

Recently, Koch and co-workers<sup>27</sup> made a comparison between experimental and calculated gas-phases as well as the conductor-like screening model (COSMO) DFT  $^{195}\text{Pt}$  chemical shifts of a series of octahedral  $[\text{PtX}_{6-n}\text{Y}_n]^{2-}$  ( $\text{X} = \text{Cl}, \text{Br}; \text{Y} = \text{F}, \text{I}$ ) complexes to assess the accuracy of computed  $^{195}\text{Pt}$  NMR chemical shifts. It was found that the discrepancies between the experimental and the DFT-calculated  $^{195}\text{Pt}$  chemical shifts vary as a function of the coordinated halide ligands, the deviation from the ideal octahedral symmetry and the Pt-X bond displacement. The speciation and hydration/solvation of  $[\text{PtX}_6]^{2-}$  ( $\text{X} = \text{Cl}, \text{Br}$ ) anions in solution have also been investigated by Koch *et al.*<sup>22</sup> employing a combination of  $^{195}\text{Pt}$  NMR together with DFT calculations and molecular dynamics (MD) simulations.

The influences of solvent effects and dynamic averaging on the  $^{195}\text{Pt}$  NMR shielding and chemical shifts of cisplatin and three cisplatin derivatives in aqueous solution were computed recently by Autschbach and co-workers<sup>28</sup> using explicit and implicit solvation models. The simulations were carried out by combining *ab initio* molecular dynamics (aiMD) simulations for the phase space sampling with all-electron relativistic NMR shielding tensor calculations using ZORA. More recently Sutter and Autschbach<sup>29</sup> studied the  $^{195}\text{Pt}$ ,  $^{14}\text{N}$ , and  $^{15}\text{N}$  NMR data for five platinum azido ( $\text{N}_3^-$ ) complexes using relativistic density functional theory (DFT). Good agreement with experiment is obtained for Pt and N chemical shifts as well as Pt-N *J*-coupling constants.

A new approach for predicting the  $^{195}\text{Pt}$  chemical shifts was proposed by Osella and co-workers.<sup>3</sup> This approach is offered by chemometrics, which tries to correlate the  $^{195}\text{Pt}$  chemical shifts from literature data to particular molecular features of an artificial neural network (ANN) algorithm. The ANN approach was applied in a series of 185 cisplatin-like complexes formulated as *cis*- $[\text{A}_2\text{PtX}_2]$  ( $\text{A}$  = amine,  $\text{A}_2$  = diamine,  $\text{X} = \text{I}, \text{Cl}$ , carboxylate,  $\text{X}_2$  = dicarboxylate).

Pickard and Mauri<sup>30</sup> performed first-principles calculations of NMR parameters using the gauge including projection augmented wave (GIPAW) method that permits the calculation of NMR chemical shifts with a pseudopotential approach. All applications to date of the GIPAW method in chemistry and materials science have recently been reviewed.<sup>31</sup> Multinuclear solid-state nuclear magnetic resonance (SSNMR) experiments have been performed by Lucier *et al.*<sup>32</sup> on cisplatin and four related square-planar compounds. The wideband uniform rate smooth truncation-Carr-Purcell-Meiboom-Gill (WURST-CPMG) pulse sequence was utilized in NMR experiments to acquire  $^{195}\text{Pt}$ ,  $^{14}\text{N}$ , and  $^{35}\text{Cl}$  ultra-wideline NMR spectra of high quality. Platinum magnetic shielding (MS) tensor orientations were calculated using both plane-wave density functional theory (DFT) and standard DFT methods. Plane-wave calculations for these systems consistently predict  $^{195}\text{Pt}$  chemical shift (CS) tensor parameters to a high degree of accuracy. The observed inconsistency of DFT calculations on isolated molecules indicated that intermolecular interactions may play a

significant role in determining the origin of the  $^{195}\text{Pt}$  CS tensor parameters and orientations.

The serendipitous discovery of the anticancer properties of cisplatin and its clinical introduction in the 1970s is generally considered to be a breakthrough in cancer treatment. In the years following the discovery of cisplatin, it has been demonstrated that the combination of transition metals with appropriate ligands can lead to clinically approved anticancer metallodrugs (carboplatin, oxaliplatin, satraplatin). The versatile physicochemical properties of the central Pt atom play a crucial role in explaining the activity against tumour cells; however, the electronic and kinetic effects of the ligands need to be considered as well.<sup>33,34</sup> An excellent publication by Boulikas *et al.*<sup>35</sup> in 2007 entitled *Designing platinum compounds in cancer: structures and mechanisms* offers an exhaustive assessment of the fertile field of the platinum anticancer drugs. Most recently Wilson and Lippard<sup>36</sup> presented an excellent overview of known synthetic strategies for the synthesis of platinum anticancer complexes.

About fifty years ago Tobe *et al.*<sup>37,38</sup> reported a detailed examination of the effect of structural variation on a range of platinum anticancer agents on the toxicity and anti-tumour properties of the compounds that they produce. Cleare and Hoeschele<sup>39,40</sup> also explored the relationships between the structure and activity of anti-tumour platinum compounds and presented the physical, chemical and structural parameters that appear to be essential for the observation of anti-tumour activity. Later on, Abdoul-Ahad and Webb<sup>41</sup> reported quantitative structure–activity relationships for some anti-tumour platinum(II) complexes using electronic indices calculated by the INDO-SCF method as independent variables. More recently Osella and co-workers<sup>42</sup> synthesized several octahedral Pt(IV) complexes of the general formula  $[\text{Pt}(\text{L})_2(\text{L}')_2(\text{L}'')_2]$  (axial ligands L are  $\text{Cl}^-$ ,  $\text{RCOO}^-$ , or  $\text{OH}^-$ ; equatorial ligands L' are two am(m)ine or one diamine; and equatorial ligands L are  $\text{Cl}^-$  or glycolato  $[\text{OCH}_2\text{COO}]^{2-}$ ) in an attempt to develop a predictive quantitative structure–activity relationship (QSAR) model. They used various physicochemical data along with calculated molecular descriptors to obtain a rigorous, externally validated QSAR with *in vitro* cytotoxicity of these “third generation” anti-tumour platinum compounds. However, the structure–activity relationship behind the high efficacy of first, second and third generation platinum anti-tumour compounds in the treatment of cancer is still not fully understood. Moreover, to the best of our knowledge, no attempts have been made so far to exploit correlations between activity, toxicity and NMR parameters, particularly the  $^{195}\text{Pt}$  NMR chemical shifts of platinum anticancer agents, as  $^{195}\text{Pt}$  NMR spectroscopy is a very useful tool for characterizing and investigating these agents.

Within this context herein we address three important issues related to the molecular and electronic structures of platinum anticancer agents in solution employing DFT methods: (i) the accurate prediction of the  $^{195}\text{Pt}$  NMR chemical shifts for a series of Pt(II) and Pt(IV) platinum anticancer agents and other relevant Pt(II) and Pt(IV) compounds based

on Gauge-Including Atomic Orbitals (GIAO) DFT calculations, hoping to contribute some much needed development of computational protocols to the difficult task of  $^{195}\text{Pt}$  NMR, (ii) the role of the conformational preferences and the solvation models employed on the calculated  $\delta$   $^{195}\text{Pt}$  chemical shifts, and (iii) the validation of non-relativistic DFT computational protocols to predict reasonably accurate  $^{195}\text{Pt}$  chemical shifts in Pt(II) and Pt(IV) coordination compounds.

## Computational details

All calculations were performed using the Gaussian 09 program suite.<sup>43</sup> The geometries of all stationary points were fully optimized, without symmetry constraints, employing the 1997 hybrid functional of Perdew, Burke and Ernzerhof<sup>44–49</sup> as implemented in the Gaussian09 program suite. This functional uses 25% exchange and 75% correlation weighting and is denoted as PBE0. For the geometry optimizations we have used the SARC-ZORA basis<sup>50,51</sup> for the Pt atom and 6-31+G(d) for all other elements E. Hereafter the method used in DFT calculations is abbreviated as PBE0/SARC-ZORA(Pt)U6-31+G(d)(E). All stationary points have been identified as minima (number of imaginary frequencies  $\text{NImag} = 0$ ). Mainly we used the Polarizable Continuum Model (PCM) using the integral equation formalism variant (IEFPCM) being the default self-consistent reaction field (SCRF) method,<sup>52</sup> and the universal continuum solvation model based on solute electron density called SMD.<sup>53</sup> Magnetic shielding tensors have been computed with the GIAO (gauge-including atomic orbitals) DFT method<sup>54,55</sup> as implemented in the Gaussian09 series of programs employing in total 25 density functionals (DFs). These are SVWN<sup>56,57</sup> in the Local Density Approximation (LDA) case, the stand-alone VSXC,<sup>58</sup> HCTH407,<sup>59–61</sup> tHCTH<sup>62</sup> and TPSS<sup>63</sup> in the Generalized Gradient Approximation (GGA) case, the hybrid B3LYP,<sup>64,65</sup> B3PW91,<sup>65</sup> mPW1PW91,<sup>66</sup> mPW3PBE,<sup>66</sup> PBE0,<sup>44–49</sup> PBEh1PBE,<sup>67</sup> HSE2PBE,<sup>68</sup> O3LYP,<sup>69</sup> X3LYP,<sup>70</sup> BMK<sup>71</sup> and B97-2,<sup>72,73</sup> in the GGA case, the global hybrids of Truhlar's Minnesota classes of functionals, M05-2X,<sup>74</sup> M06-2X<sup>75</sup> and M06-L,<sup>76</sup> the BP86<sup>77–79</sup> in the local GGA case, the BB95<sup>80</sup> and TPSS<sup>81</sup> in the local *meta*-GGA case and the long range corrected LC-wPBE,<sup>82–85</sup> CAM-B3LYP<sup>86</sup> and wB97XD<sup>87</sup> functionals. To be consistent with the experimental data available we report  $^{195}\text{Pt}$  NMR chemical shifts with respect to either the  $[\text{PtCl}_4]^{2-}$  (aq) or the  $[\text{PtCl}_6]^{2-}$  (aq) reference compounds, using the chemical shift definition:<sup>88</sup>

$$\delta = (\sigma_{\text{ref}} - \sigma) / (1 - \sigma_{\text{ref}})$$

in its approximate form:

$$\delta \approx (\sigma_{\text{ref}} - \sigma)$$

Shielding constants and chemical shifts are given in ppm.

## Results and discussion

### 1. $^{195}\text{Pt}$ NMR of the $[\text{PtCl}_6]^{2-}$ reference compound

It is well established that structural effects combined with the presence of a solvent influence significantly the  $^{195}\text{Pt}$  NMR parameters.<sup>2,13,25</sup> Therefore we optimized the structure of the  $[\text{PtCl}_6]^{2-}$  reference compound at various levels of theory in aqueous solution employing the PCM solvation model.

The isotropic shielding tensor elements,  $\sigma^{\text{iso}} \text{ } ^{195}\text{Pt}$  (ppm), of the  $[\text{PtCl}_6]^{2-}$  reference in aqueous solution calculated at various levels of theory are shown pictorially in Chart 1. Note that the resonance for  $[\text{PtCl}_6]^{2-} = -1628$  ppm, whereas  $[\text{PtCl}_6]^{2-} = 1628$  ppm.<sup>2</sup>

An inspection of Chart 1 reveals that the PBE0 DF provides the most accurate predictions of the  $\sigma^{\text{iso}} \text{ } ^{195}\text{Pt}$  (ppm) of the  $[\text{PtCl}_6]^{2-}$  reference compound in aqueous solution (the deviation from the experimental value is only  $-1.1\%$ ). The mPW1PW91 and B97-2 DFs also perform well; the deviations from the experimental values amount to  $3.7\%$  for the mPW1PW91 DF and to  $-3.1\%$  for the B97-2 functional. Good agreement between theory and experiment is also obtained by the popular B3LYP DF, the percentage deviations being  $7.9$  and  $-6.8$  for the  $[\text{PtCl}_6]^{2-}$  and  $[\text{PtCl}_4]^{2-}$  complexes, respectively. The worst results are obtained by Minnesota's, M05-2X, M06-2X and M06-L DFs. The structural and  $^{195}\text{Pt}$  NMR parameters of the  $[\text{PtCl}_6]^{2-}$  calculated at various levels of theory in

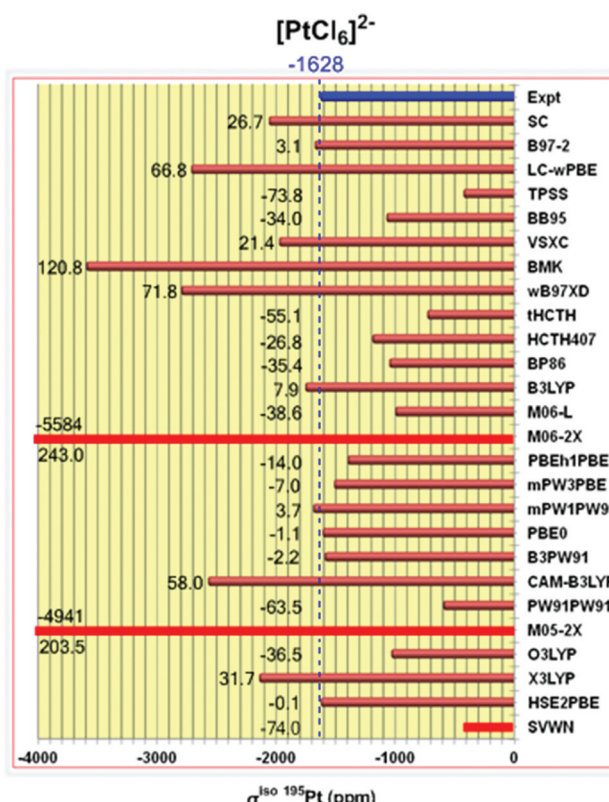


Chart 1 The isotropic shielding tensor elements,  $\sigma^{\text{iso}} \text{ } ^{195}\text{Pt}$  (ppm), of the  $[\text{PtCl}_6]^{2-}$  reference in aqueous solution calculated at various levels of theory.

Table 1 The estimated Pt–Cl bond lengths (in Å) and  $\sigma^{\text{iso}} \text{ } ^{195}\text{Pt}$  (ppm) of the  $[\text{PtCl}_6]^{2-}$  reference compound calculated at the PBE0/SARC-ZORA (Pt)U6-31G(d,p)(Cl) level employing the PCM and SMD solvation models

Solvent	Pt–Cl		$\sigma^{\text{iso}} \text{ } ^{195}\text{Pt}$	
	PCM	SMD	PCM	SMD
Water	2.396	2.396	-1600	-1680
DMF	2.396	2.396	-1591	-1676
DMSO	2.392	2.394	-1539	-1663
Methanol	2.393	2.394	-1566	-1666
Chloroform	2.394	2.398	-1702	-1787
Acetone	2.392	2.395	-1571	-1690
CP-aiMD <sup>a</sup>	$2.385 \pm 0.021$		$-2063 \pm 44^b$	

<sup>a</sup> Car-Parrinello *ab initio* molecular dynamics (CP-aiMD) simulation, ref. 25. <sup>b</sup> Scalar relativistic ZORA calculations, ref. 25.

aqueous solutions along with the percent deviations from the experimental data are given in ESI (Table S1†). Therefore PBE0 was our choice to calculate the  $\delta \text{ } ^{195}\text{Pt}$  (ppm) chemical shifts of the Pt(II) and Pt(IV) compounds under study.

Next we explored the solvent effects in conjunction with the PCM and SMD solvation models used on the structural parameters and the isotropic shielding tensor elements  $\sigma^{\text{iso}} \text{ } ^{195}\text{Pt}$  of the  $[\text{PtCl}_6]^{2-}$  reference compound. The estimated Pt–Cl bond lengths and the  $\sigma^{\text{iso}} \text{ } ^{195}\text{Pt}$  values of  $[\text{PtCl}_6]^{2-}$  are compiled in Table 1.

It can be seen that the  $[\text{PtCl}_6]^{2-}$  and  $[\text{PtCl}_4]^{2-}$  complexes retain the octahedral and square planar geometries in solution. The estimated Pt–Cl bond distances at various levels of theory (Table S1†) were found in the range 2.363–2.445 Å and 2.370–2.464 Å for  $[\text{PtCl}_6]^{2-}$  and  $[\text{PtCl}_4]^{2-}$  respectively. Generally, independently of the DFs employed, solvation of the complexes causes elongation of the Pt–Cl bonds by 0.047–0.129 Å and 0.055–0.149 Å in  $[\text{PtCl}_6]^{2-}$  and  $[\text{PtCl}_4]^{2-}$  complexes, respectively. The polar nature of the Pt–Cl bonds accounts well for their elongation upon solvation by polar solvents. The Pt–Cl distances for  $[\text{PtCl}_6]^{2-}$  calculated at the PBE0/SARC-ZORA (Pt)U6-31G(d,p)(Cl) level employing either the PCM or the SMD solvation model are in good agreement with those obtained by the CP-aiMD calculations (2.385 ± 0.021 Å).<sup>25</sup> It can also be seen that both solvent and solvation models have practically no effect on the Pt–Cl bond distances. The changes of the Pt–Cl bond lengths observed are up to 0.004 Å. However, both solvent and solvation models influence the estimated  $\sigma^{\text{iso}} \text{ } ^{195}\text{Pt}$  of  $[\text{PtCl}_6]^{2-}$ . Depending on the solvent used, changes of  $\sigma^{\text{iso}} \text{ } ^{195}\text{Pt}$  values up to 163 ppm are observed. The solvation model also affects significantly the calculated  $\sigma^{\text{iso}} \text{ } ^{195}\text{Pt}$  shielding tensor elements. The calculated  $\sigma^{\text{iso}} \text{ } ^{195}\text{Pt}$  values employing the SMD solvation model are 80–124 ppm lower than those obtained with the PCM solvation model, the differences observed depending on the solvent used.

### 2. Performance of the DFs in the calculation of $^{195}\text{Pt}$ NMR of some representative square planar Pt(II) and octahedral Pt(IV) complexes

We further test and validate the various computational protocols by calculating the  $^{195}\text{Pt}$  NMR chemical shifts of some

representative square planar Pt(II) ( $[\text{PtCl}_4]^{2-}$ ,  $[\text{PtBr}_4]^{2-}$ ,  $[\text{Pt}(\text{CN})_4]^{2-}$ ,  $[\text{Pt}(\text{NH}_3)_3\text{Cl}]^+$ ,  $[\text{Pt}(\text{NH}_3)_3\text{Br}]^+$ ,  $[\text{Pt}(\text{NH}_3)_3\text{I}]^+$ ,  $[\text{Pt}(\text{NH}_3)_3(\text{OH})]^+$  and  $[\text{Pt}(\text{NH}_3)_4]^{2+}$ ) and octahedral Pt(IV) ( $[\text{PtF}_6]^{2-}$ ,  $[\text{PtBr}_6]^{2-}$ ,  $[\text{PtI}_6]^{2-}$ , *cis*- $[\text{PtCl}_4\text{Br}_2]^{2-}$ , *cis*- $[\text{PtCl}_2\text{Br}_4]^{2-}$ ,  $[\text{PtCl}_5(\text{OH})]^{2-}$  and  $[\text{Pt}(\text{OH})_6]^{2-}$ ) complexes. The estimated  $\delta^{195}\text{Pt}$  (ppm) chemical shifts of the square planar Pt(II) and octahedral Pt(IV) complexes referenced to  $[\text{PtCl}_6]^{2-}$  calculated with various computational protocols in aqueous solution are shown pictorially in Charts 2 and 3 respectively. The percentage deviations from the experimental values for the good performer DFs are also given in Charts 2 and 3.

As one can see from Chart 2, among the DFs employed, PBE0, CAM-B3LYP and X3LYP predict  $^{195}\text{Pt}$  NMR chemical shifts for the eight diverse square planar Pt(II) complexes in close agreement with experiment. The percentage deviations from the experimental values (Chart 2) are 3.4%, 1.2%, -8.8%, -3.4%, 0.5%, -0.8%, 10.5% and -3.3% for PBE0, 8.8%, 7.5%, 3.0%, -7.5%, 3.5%, 0.4%, 19.6% and -1.3% for CAM-B3LYP, and -1.4%, -0.1%, -15.2%, -16.1%, -5.4%, -5.5%, -2.3% and 18.6% for X3LYP for the square planar  $[\text{PtCl}_4]^{2-}$ ,  $[\text{PtBr}_4]^{2-}$ ,  $[\text{Pt}(\text{CN})_4]^{2-}$ ,  $[\text{Pt}(\text{NH}_3)_3\text{Cl}]^+$ ,  $[\text{Pt}(\text{NH}_3)_3\text{Br}]^+$ ,  $[\text{Pt}(\text{NH}_3)_3\text{I}]^+$ ,  $[\text{Pt}(\text{NH}_3)_3(\text{OH})]^+$  and  $[\text{Pt}(\text{NH}_3)_4]^{2+}$  complexes, respectively. It can also be seen that PBE0 shows the best performance for the set of eight square planar Pt(II) complexes predicting  $^{195}\text{Pt}$  NMR chemical shifts in excellent agreement with experiment (percentage deviations less than 10.5%).

Perusal of Chart 3 reveals that PBE0 is again the best performer for the prediction of the  $^{195}\text{Pt}$  NMR chemical shifts of the  $[\text{PtF}_6]^{2-}$ ,  $[\text{PtBr}_6]^{2-}$ ,  $[\text{PtI}_6]^{2-}$ , *cis*- $[\text{PtCl}_4\text{Br}_2]^{2-}$ , *cis*- $[\text{PtCl}_2\text{Br}_4]^{2-}$ ,  $[\text{PtCl}_5(\text{OH})]^{2-}$  and  $[\text{Pt}(\text{OH})_6]^{2-}$  octahedral Pt(IV) complexes with percentage deviations from experiment of 15.8%, 2.2%, 6.1%, 9.0%, 4.7%, 5.8% and -3.3%, respectively. It is noteworthy that, with the exception of the  $[\text{PtF}_6]^{2-}$  complex, the percentage deviations are less than 9.0%. In all cases, Minnesota's, M05-2X, M06-2X and M06-L DFs are the worst performers in predicting the  $^{195}\text{Pt}$  NMR chemical shifts of the square planar Pt(II) and octahedral Pt(IV) complexes. It is important to note that the percentage deviations of  $^{195}\text{Pt}$  chemical shifts from experiment are -10.4%, -0.3%, -1.0%, -2.6%, -3.1%, 1.2% and -20.5% for the  $[\text{PtF}_6]^{2-}$ ,  $[\text{PtBr}_6]^{2-}$ ,  $[\text{PtI}_6]^{2-}$ , *cis*- $[\text{PtCl}_4\text{Br}_2]^{2-}$ , *cis*- $[\text{PtCl}_2\text{Br}_4]^{2-}$ ,  $[\text{PtCl}_5(\text{OH})]^{2-}$  and  $[\text{Pt}(\text{OH})_6]^{2-}$  octahedral Pt(IV) complexes, respectively, calculated at the spin-orbit ZORA relativistic level employing the COSMO solvation model.<sup>22,27</sup> A comparison of the results obtained reveals that the non-relativistic GIAO-PBE0/SARC-ZORA(Pt)U6-31+G(d)(E) computational protocol performs equally well with the spin-orbit ZORA relativistic one. Considering the high sensitivity of the  $^{195}\text{Pt}$  chemical shifts to relativistic and spin orbit effects, the good performance of the non-relativistic GIAO-PBE0/SARC-ZORA(Pt)U6-31+G(d)(E) computational protocol might be due to effective error compensation. Moreover, when relative  $\delta(^{195}\text{Pt})$  chemical shifts, *i.e.* differences between shielding tensor elements of the reference and the probe, are considered, scalar relativistic effects are attenuated because the shielding contributions from the inner cores are quite similar and tend to cancel to a large extent in the  $d$  values.<sup>89</sup>

### 3. Performance of the DFs in the calculation of $^{195}\text{Pt}$ NMR of representative anticancer square planar Pt(II) agents

It is instructive to further test and validate the various computational protocols employed by calculating the  $^{195}\text{Pt}$  NMR chemical shifts for selected representative anticancer Pt(II) complexes formulated as *cis*-(amine)<sub>2</sub>PtX<sub>2</sub>. The estimated  $\delta^{195}\text{Pt}$  (ppm) chemical shifts referenced to  $[\text{PtCl}_4]^{2-}$  ( $\sigma_{\text{ref}}^{\text{iso}} = -3294$  ppm calculated at the GIAO-PBE0/SARC-ZORA(Pt)U6-31+G(d)(E)//M05-2X/SARC-ZORA(Pt)U6-31+G(d)(E) level using the Gaussian 03 program suite for all attempts to locate the minimum structure for  $[\text{PtCl}_4]^{2-}$  using the Gaussian 09 program suite were unsuccessful) in aqueous solution calculated with various computational protocols are shown pictorially in Chart 4.

Perusal of Chart 4 reveals that PBE0 is again the best performer for the prediction of the  $^{195}\text{Pt}$  NMR chemical shifts of the *cis*-(amine)<sub>2</sub>PtX<sub>2</sub> complexes with percentage deviations from experiment of 4.2%, -3.2%, -5.7%, -11.8%, -1.3% and 3.6% for the *cis*-(NH<sub>3</sub>)<sub>2</sub>PtCl<sub>2</sub>, *cis*-(MeNH<sub>2</sub>)<sub>2</sub>PtCl<sub>2</sub>, *cis*-(<sup>i</sup>PrNH<sub>2</sub>)<sub>2</sub>PtCl<sub>2</sub>, *cis*-[(C<sub>3</sub>H<sub>5</sub>)NH<sub>2</sub>]<sub>2</sub>PtCl<sub>2</sub>, *cis*-(NH<sub>3</sub>)<sub>2</sub>PtBr<sub>2</sub> and *cis*-(NH<sub>3</sub>)<sub>2</sub>PtI<sub>2</sub> complexes, respectively. The higher percentage deviation of -11.8% observed for the *cis*-[(C<sub>3</sub>H<sub>5</sub>)NH<sub>2</sub>]<sub>2</sub>PtCl<sub>2</sub> complex could be attributed to the high sensitivity of the  $^{195}\text{Pt}$  NMR chemical shifts to conformational changes, a fact which will be discussed in the following section. It should be noticed that the percentage deviations from experiment of the aiMD averaged  $^{195}\text{Pt}$  NMR chemical shifts for the *cis*-(NH<sub>3</sub>)<sub>2</sub>PtCl<sub>2</sub> and *cis*-(NH<sub>3</sub>)<sub>2</sub>PtBr<sub>2</sub> complexes computed at the spin-orbit ZORA level of theory<sup>28</sup> are 8.6% and 9.6% respectively, illustrating once again the good performance of the non-relativistic GIAO-PBE0/SARC-ZORA(Pt)U6-31+G(d)(E) computational protocol.

### 4. Accurate prediction of $^{195}\text{Pt}$ NMR of square planar *cis*-(amine)<sub>2</sub>PtX<sub>2</sub> (X = Cl, Br, I) anticancer agents. The crucial role of conformation

In light of the good overall performance of the PBE0 DF for the calculation of the  $^{195}\text{Pt}$  NMR chemical shifts of Pt(II) and Pt(IV) complexes, we calculated the  $^{195}\text{Pt}$  NMR chemical shifts for a wide range of *cis*-(amine)<sub>2</sub>PtX<sub>2</sub> (X = Cl, Br, I) anticancer agents (in total 42 complexes) employing the GIAO-PBE0/SARC-ZORA(Pt)U6-31+G(d)(E) (E = main group element) computational protocol. The selection of the 6-31+G(d) basis set for the main group elements E was based on the exhaustive investigation of the role of the basis set in the prediction of the structure and reactivity of cisplatin and its hydrolysis products reported recently.<sup>90</sup> Calculations were performed for solutions of the complexes in DMF; for the experimental data available in the literature refer to DMF solutions of the complexes. A series of calculations was performed to investigate the sensitivity of the  $^{195}\text{Pt}$  NMR chemical shifts to conformational changes resulting from the free rotation of the amine ligands around the Pt-N bond of the anticancer agents. The torsional energy curves along the diabatic (unrelaxed) rotation around the Pt-N bond of representative *cis*-(amine)<sub>2</sub>PtCl<sub>2</sub> anticancer agents computed at the PBE0/SARC-ZORA(Pt)U6-31+G(d)(E)

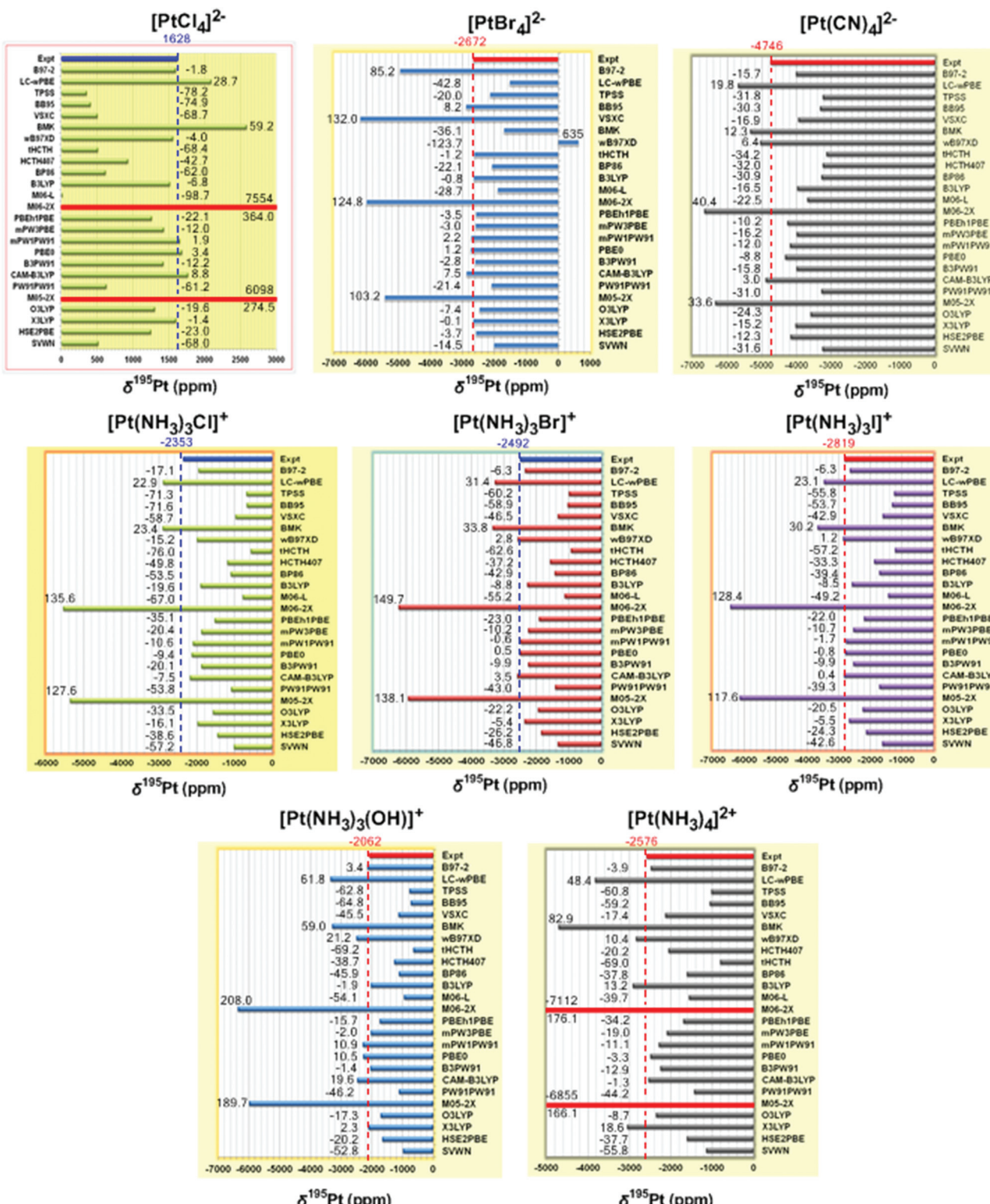
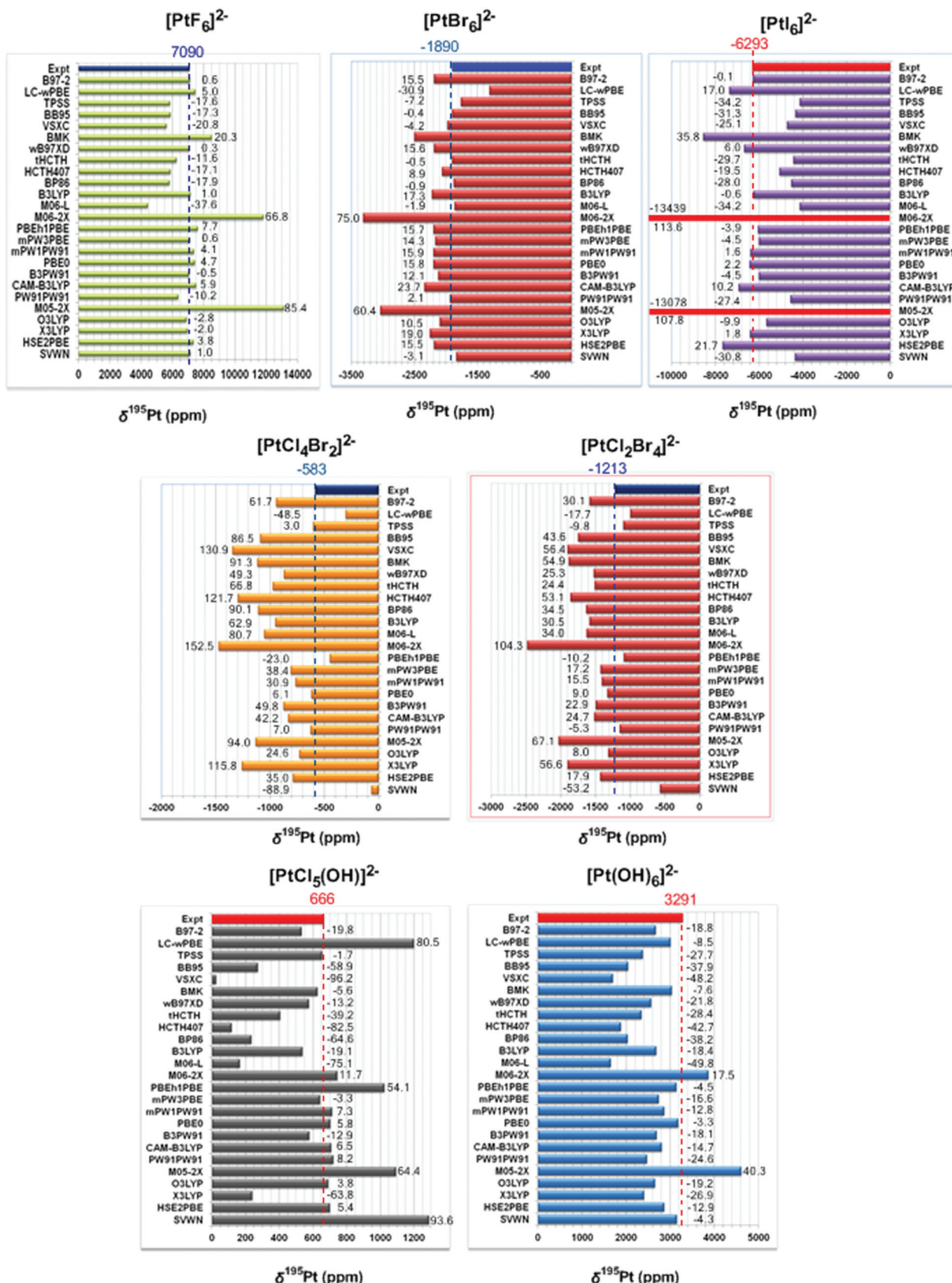


Chart 2  $\delta^{195}\text{Pt}$  (ppm) chemical shifts of square planar Pt(II) complexes referenced to  $[\text{PtCl}_4]^{2-}$  in aqueous solution calculated at various levels of theory. The numbers listed in the chart are the percentage deviations from the experimental values.

level are shown in Fig. 1. Selected structural parameters and the  $^{195}\text{Pt}$  NMR chemical shifts for a large set of Pt(II) anti-cancer agents are given in Table 2. The experimental  $^{195}\text{Pt}$

NMR chemical shifts available<sup>1–4,91,92</sup> along with the percentage deviation of the calculated from the experimental values are also given in Table 2.



**Chart 3**  $\delta^{195}\text{Pt}$  (ppm) chemical shifts of octahedral Pt(iv) complexes referenced to  $[\text{PtCl}_6]^{2-}$  in aqueous solution calculated at various levels of theory. The numbers listed in the chart are the percentage deviations from the experimental values.

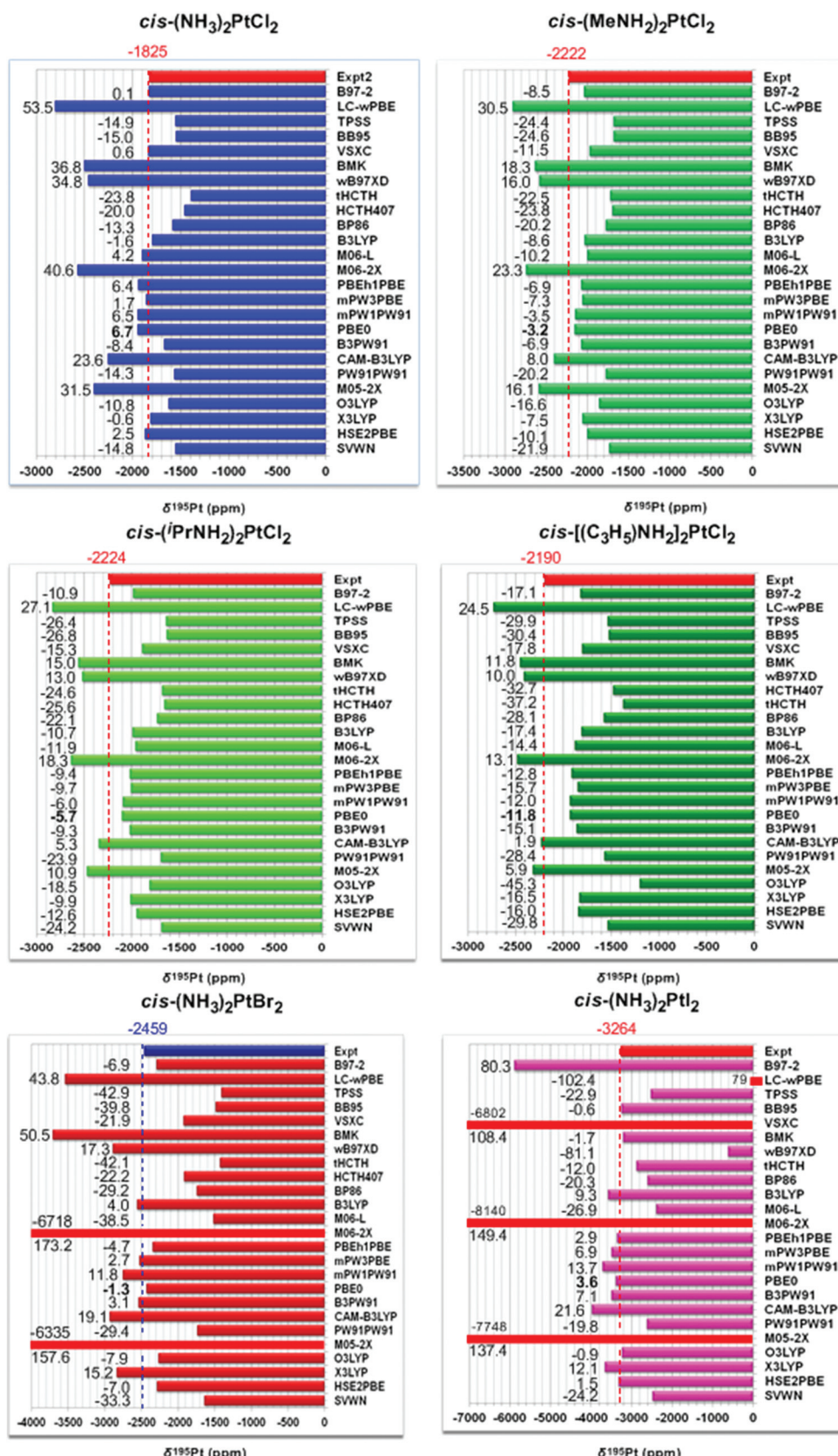


**Chart 4**  $\delta^{195}\text{Pt}$  (ppm) chemical shifts of representative anticancer square planar Pt(II) complexes referenced to  $[\text{PtCl}_4]^{2-}$  in aqueous solution calculated at various levels of theory. The numbers listed in the chart are the percentage deviations from the experimental values.

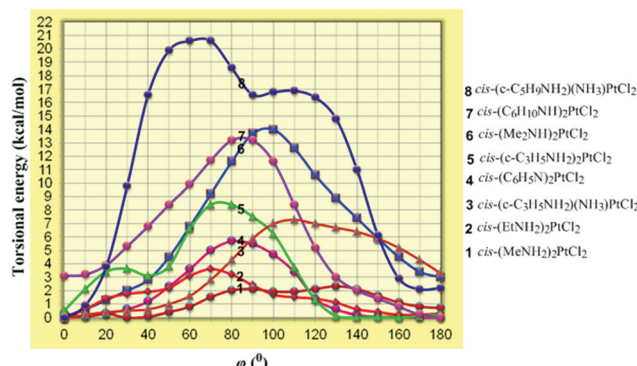


**Fig. 1** Torsional energy curves along the diabatic (unrelaxed) rotation around the Pt–N bond of representative *cis*-(amine)<sub>2</sub>PtCl<sub>2</sub> anticancer agents computed at the PBE0/SARC-ZORA(Pt)U6-31+G(d)(E) level.

As expected DMF solvation of the complexes causes elongation of the Pt–N and Pt–Cl bonds by 0.08–0.14 Å and 0.09–0.11 Å respectively in comparison with the available experimentally determined X-ray structures of the *cis*-(C<sub>5</sub>H<sub>10</sub>NH)<sub>2</sub>PtCl<sub>2</sub>,<sup>93</sup> *cis*-(C<sub>5</sub>H<sub>10</sub>NH)<sub>2</sub>PtCl<sub>2</sub>,<sup>94</sup> *cis*-(C<sub>6</sub>H<sub>11</sub>NH<sub>2</sub>)<sub>2</sub>PtCl<sub>2</sub>,<sup>95</sup> and *cis*-(C<sub>6</sub>H<sub>11</sub>NH<sub>2</sub>)(NH<sub>3</sub>)PtCl<sub>2</sub><sup>96</sup> complexes. Similarly, the N–Pt–N and Cl–Pt–Cl bond angles are opened by 2.2–6.9 and 0.4–3.2° respectively upon DMF solvation. The observed elongation of the Pt–N and Pt–Cl bonds upon solvation by polar solvents could be explained by the polar nature of the Pt–N and Pt–Cl bonds and the increase of the coordination number of the complexes through the coordination of solvent molecules.

It is noteworthy that the *cis*-(amine)<sub>2</sub>PtX<sub>2</sub> (X = Cl, Br, I) anticancer agents in DMF solutions adopt various conformations due to the “free” rotation of the amine ligands around the Pt–N bond surmounting very low torsional barriers (Fig. 1). The most important finding is the *high sensitivity of the* <sup>195</sup>Pt NMR chemical shifts to conformational changes induced by the free rotation of the amine ligands around the Pt–N bond of the anticancer agents. The changes of the isotropic shielding tensor elements ( $\sigma^{iso}$ ) observed along the diabatic (unrelaxed) rotation around the Pt–N bond are found to be in the range 50–1009 ppm (cf. Table S2 in ESI†). These changes could be attributed to the changes of the overlap population of the Pt–N bond introduced by the rotation that affects the electron density on the Pt central atom. This could be the reason for the difficulties encountered in the accurate prediction of the <sup>195</sup>Pt chemical shifts in solution employing electronic structure calculation methods. A clear demonstration of the effect of the conformational changes on the electron density of the Pt central atom and consequently on the calculated  $\sigma^{iso}$ (<sup>195</sup>Pt) shielding tensor elements is given in Fig. 2 for the torsional rotation of a representative *cis*-(C<sub>5</sub>H<sub>5</sub>N)<sub>2</sub>PtCl<sub>2</sub> anticancer agent around the Pt–N bond.

An inspection of the calculated  $\delta_{calcd}^{195}\text{Pt}$  and experimental  $\delta_{expt}^{195}\text{Pt}$  chemical shifts given in Table 2 reveals the

excellent performance of the GIAO-PBE0/SARC-ZORA(Pt)U6-31+G(d)(E) computational protocol (the mean percentage deviation of the calculated from the experimental values is around −2.8%). Generally this computational protocol underestimates the  $\delta^{195}\text{Pt}$  chemical shifts with respect to the experimental values by −0.3 up to −6.0%. Exceptions are the calculated  $\delta^{195}\text{Pt}$  chemical shifts for the *cis*-(C<sub>4</sub>H<sub>7</sub>NH<sub>2</sub>)<sub>2</sub>PtCl<sub>2</sub>, *cis*-(2-Adamantamine)<sub>2</sub>PtCl<sub>2</sub>, *cis*-(C<sub>5</sub>H<sub>9</sub>NH<sub>2</sub>)(NH<sub>3</sub>)PtCl<sub>2</sub>, (1,2-DACH)-PtCl<sub>2</sub>, *cis*-(NH<sub>3</sub>)<sub>2</sub>PtBr<sub>2</sub>, *cis*-(NH<sub>3</sub>)<sub>2</sub>PtI<sub>2</sub> and *cis*-(C<sub>5</sub>H<sub>5</sub>N)<sub>2</sub>PtI<sub>2</sub> which are overestimated by 1.1%, 1.2%, 1.3%, 1.1%, 2.4%, 2.7% and 4.7%, respectively.

The excellent performance of the computational protocol employed in the calculation of the  $\delta^{195}\text{Pt}$  chemical shifts is also mirrored on the plot of  $\delta_{expt}^{195}\text{Pt}$  vs.  $\delta_{calcd}^{195}\text{Pt}$  chemical shifts of the *cis*-(amine)<sub>2</sub>PtX<sub>2</sub> (X = Cl, Br, I) anticancer agents shown in Fig. 3.

The plot of  $\delta_{expt}^{195}\text{Pt}$  vs.  $\delta_{calcd}^{195}\text{Pt}$  chemical shifts illustrates further the excellent agreement of the calculated with the experimental values. The calculated values are typically 99% of the experimental ones (setting the intercept to zero, the linear relationship becomes  $\delta_{expt}^{195}\text{Pt} = 0.99\delta_{calcd}^{195}\text{Pt}$  with  $R^2 = 0.958$ ).

The crucial role of the conformational preferences on the electron density of the Pt central atom and consequently on the  $\delta_{calcd}^{195}\text{Pt}$  chemical shifts was further corroborated by the plots of the  $\delta_{calcd}^{195}\text{Pt}$  chemical shifts vs. the natural atomic charge  $Q_{\text{Pt}}$  given in Fig. 4.

Noteworthy is the good linear relationship between  $\delta_{calcd}^{195}\text{Pt}$  and  $Q_{\text{Pt}}$  ( $R^2 = 0.903$ ) for the complete set of *cis*-(amine)<sub>2</sub>PtX<sub>2</sub> (X = Cl, Br, I) anticancer agents under consideration. Note that the linear relationships between  $\delta_{calcd}^{195}\text{Pt}$  and  $Q_{\text{Pt}}$  become better for the subset of complexes with analogous steric hindrance effects (A and B in Fig. 4) and become worst for the subset of complexes with different steric hindrance effects (C in Fig. 4).

##### 5. Do $\delta_{calcd}^{195}\text{Pt}$ chemical shifts correlate with the $pK_a$ of the protonated amine ligands?

It would be interesting to plot the  $\delta_{calcd}^{195}\text{Pt}$  chemical shifts of the *cis*-(amine)<sub>2</sub>PtCl<sub>2</sub> complexes against the  $pK_a$  values of the protonated amines. This could bring a better understanding of how steric hindrance and solvent effects are related to the chemical shifts. Table 3 shows the  $\delta_{calcd}^{195}\text{Pt}$  chemical shifts along with the  $(pK_a)_w$  and  $(pK_a)_{AN}$  values for the amines available so far (subscripts w and AN denote water and acetonitrile solutions).<sup>97</sup>

A study of the correlation between the  $\delta_{calcd}^{195}\text{Pt}$  chemical shifts and the  $(pK_a)_w$  and  $(pK_a)_{AN}$  of the protonated amines was performed and excellent linear relationships were observed (Fig. 5).

Accordingly the  $\delta_{calcd}^{195}\text{Pt}$  chemical shifts correlate linearly with the  $pK_a$  of the protonated amine ligands. Including in the correlations the data for the outlier *cis*-[(CH<sub>3</sub>)<sub>2</sub>NH]<sub>2</sub>PtCl<sub>2</sub> complex the linear relationships  $\delta_{calcd}^{195}\text{Pt} = -53.43(pK_a)_w - 1619.6$  ( $R^2 = 0.886$ ) and  $\delta_{calcd}^{195}\text{Pt} = -47.43(pK_a)_{AN} - 1317.6$  ( $R^2 = 0.873$ ) were obtained. The lower  $R^2$  values indicate that

**Table 2** Selected structural parameters (bond lengths in Å, bond angles in degrees) and the  $^{195}\text{Pt}$  NMR chemical shifts (in ppm) for a large set of *cis*-(amine)<sub>2</sub>PtX<sub>2</sub> (X = Cl, Br, I) anticancer agents referenced to [PtCl<sub>4</sub>]<sup>2-</sup> ( $\delta_{\text{ref}}^{\text{iso}} = -3294$  ppm) calculated at the GIAO-PBE0/SARC-ZORA(Pt)U6-31+G(d)-E//PBE0/SARC-ZORA(Pt)U6-31+G(d)(E) level in DMF solutions

Compound	$R_{\text{Pt}-\text{Cl}}$	$R_{\text{Pt}-\text{N}}$	<N-Pt-N	<Cl-Pt-Cl	$\delta^{(195)\text{Pt}}$ (ppm)		
					Calcd	Expt	Dev. (%)
<i>cis</i> -(NH <sub>3</sub> ) <sub>2</sub> PtCl <sub>2</sub>	2.400	2.136	92.2	94.2	-2076	-2097	-1.0
<i>trans</i> -(NH <sub>3</sub> ) <sub>2</sub> PtCl <sub>2</sub>	2.417	2.119	180.0	180.0	-2161	-2174	-0.6
<i>cis</i> -(CH <sub>3</sub> NH <sub>2</sub> ) <sub>2</sub> PtCl <sub>2</sub>	2.403	2.145	93.7	93.8	-2210	-2222	-0.5
<i>cis</i> -(C <sub>2</sub> H <sub>5</sub> NH <sub>2</sub> ) <sub>2</sub> PtCl <sub>2</sub>	2.405	2.145	93.3	94.1	-2196	—	—
<i>cis</i> -(n-C <sub>3</sub> H <sub>7</sub> NH <sub>2</sub> ) <sub>2</sub> PtCl <sub>2</sub>	2.404	2.145	93.1	93.9	-2219	—	—
<i>cis</i> -(n-C <sub>4</sub> H <sub>9</sub> NH <sub>2</sub> ) <sub>2</sub> PtCl <sub>2</sub>	2.406	2.144	93.4	93.9	-2224	—	—
<i>cis</i> -(n-C <sub>5</sub> H <sub>11</sub> NH <sub>2</sub> ) <sub>2</sub> PtCl <sub>2</sub>	2.404	2.145	93.2	94.0	-2210	—	—
<i>cis</i> -(n-C <sub>6</sub> H <sub>13</sub> NH <sub>2</sub> ) <sub>2</sub> PtCl <sub>2</sub>	2.409	2.145	93.8	94.1	-2161	-2215 <sup>a</sup>	-2.4
<i>cis</i> -(n-C <sub>7</sub> H <sub>15</sub> NH <sub>2</sub> ) <sub>2</sub> PtCl <sub>2</sub>	2.409	2.145	94.0	94.2	-2151	—	—
<i>cis</i> -(n-C <sub>8</sub> H <sub>17</sub> NH <sub>2</sub> ) <sub>2</sub> PtCl <sub>2</sub>	2.408	2.144	93.4	94.1	-2179	—	—
<i>cis</i> -(i-PrNH <sub>2</sub> ) <sub>2</sub> PtCl <sub>2</sub>	2.411	2.153	95.2	93.3	-2132	-2224	-4.3
<i>cis</i> -(i-BuNH <sub>2</sub> ) <sub>2</sub> PtCl <sub>2</sub>	2.408	2.148	94.3	94.1	-2140	—	—
<i>cis</i> -(i-AmNH <sub>2</sub> ) <sub>2</sub> PtCl <sub>2</sub>	2.409	2.140	93.1	94.5	-2221	—	—
<i>cis</i> -(c-C <sub>3</sub> H <sub>5</sub> NH <sub>2</sub> ) <sub>2</sub> PtCl <sub>2</sub>	2.410	2.150	94.3	93.9	-2098	-2190	-4.2
<i>cis</i> -(c-C <sub>4</sub> H <sub>7</sub> NH <sub>2</sub> ) <sub>2</sub> PtCl <sub>2</sub>	2.407	2.149	93.9	93.6	-2249	-2225	1.1
<i>cis</i> -(c-C <sub>5</sub> H <sub>9</sub> NH <sub>2</sub> ) <sub>2</sub> PtCl <sub>2</sub>	2.408	2.152	93.9	93.6	-2190	-2204	-0.6
<i>cis</i> -(c-C <sub>6</sub> H <sub>11</sub> NH <sub>2</sub> ) <sub>2</sub> PtCl <sub>2</sub>	2.412	2.161	95.2	92.8	-2191	-2208	-0.8
<i>cis</i> -(c-C <sub>7</sub> H <sub>13</sub> NH <sub>2</sub> ) <sub>2</sub> PtCl <sub>2</sub>	2.412	2.152	94.7	93.4	-2125	—	—
<i>cis</i> -(c-C <sub>8</sub> H <sub>15</sub> NH <sub>2</sub> ) <sub>2</sub> PtCl <sub>2</sub>	2.409; 2.412	2.154; 2.163	92.6	92.1	-2119	—	—
<i>cis</i> -(1-Adamantamine) <sub>2</sub> PtCl <sub>2</sub>	2.412	2.159	94.7	92.6	-2099	-2184	-3.9
<i>cis</i> -(2-Adamantamine) <sub>2</sub> PtCl <sub>2</sub>	2.409	2.168	94.3	93.3	-2256	-2230	1.2
<i>cis</i> -(C <sub>5</sub> H <sub>5</sub> N) <sub>2</sub> PtCl <sub>2</sub>	2.403	2.122	89.6	92.7	-1907	-1965	-2.9
<i>cis</i> -(C <sub>5</sub> H <sub>10</sub> NH) <sub>2</sub> PtCl <sub>2</sub>	2.417	2.162	92.3	92.2	-2234	-2282	-2.1
<i>cis</i> [(CH <sub>3</sub> ) <sub>2</sub> NH] <sub>2</sub> PtCl <sub>2</sub>	2.414	2.172	90.4	91.1	-2128	-2188	-2.8
<i>cis</i> -(CH <sub>3</sub> NH <sub>2</sub> ) <sub>2</sub> [NH <sub>3</sub> ]PtCl <sub>2</sub>	2.402; 2.405	2.136; 2.144	93.1	94.1	-2108	-2186	-3.6
<i>cis</i> -(i-PrNH <sub>2</sub> )(NH <sub>3</sub> )PtCl <sub>2</sub>	2.405; 2.406	2.145; 2.146	92.8	93.9	-2066	-2162	-4.4
<i>cis</i> -(c-C <sub>3</sub> H <sub>5</sub> NH <sub>2</sub> )(NH <sub>3</sub> )PtCl <sub>2</sub>	2.404; 2.404	2.141; 2.145	92.9	94.2	-2070	-2145	-3.5
<i>cis</i> -(c-C <sub>4</sub> H <sub>7</sub> NH <sub>2</sub> )(NH <sub>3</sub> )PtCl <sub>2</sub>	2.401; 2.406	2.143; 2.145	92.5	93.8	-2196	-2168	1.3
<i>cis</i> -(c-C <sub>5</sub> H <sub>9</sub> NH <sub>2</sub> )(NH <sub>3</sub> )PtCl <sub>2</sub>	2.402; 2.404	2.145; 2.154	93.2	93.5	-2100	-2158	-2.7
<i>cis</i> -(c-C <sub>6</sub> H <sub>11</sub> NH <sub>2</sub> )(NH <sub>3</sub> )PtCl <sub>2</sub>	2.403; 2.409	2.146; 2.155	93.2	93.3	-2039	-2162	-5.7
<i>cis</i> -(Quinoline)(NH <sub>3</sub> )PtCl <sub>2</sub>	2.396; 2.400	2.133; 2.139	91.0	93.3	-1913	-2035	-6.0
(H <sub>2</sub> NCH <sub>2</sub> CH <sub>2</sub> NH <sub>2</sub> )PtCl <sub>2</sub>	2.406	2.132	81.8	94.3	-2302	-2345	-1.8
[H <sub>2</sub> NCH <sub>2</sub> CH <sub>2</sub> NH(CH <sub>2</sub> CH <sub>2</sub> OH)]PtCl <sub>2</sub>	2.406	2.126; 2.152	82.9	94.1	-2278	-2360	-3.5
[MeHNCH <sub>2</sub> CH <sub>2</sub> NHMe]PtCl <sub>2</sub>	2.406	2.143	83.3	93.9	-2329	-2433	-4.3
(1,2-DACH)PtCl <sub>2</sub> <sup>b</sup>	2.409	2.123	81.3	94.4	-2313	-2287	1.1
(1,4-DACH)PtCl <sub>2</sub> <sup>c</sup>	2.409	2.147	97.7	94.1	-2201	-2208	-0.3
(1,2-DACH)PtCl(Gua) <sup>d</sup>	2.409	2.108; 2.136	81.2	95.0	-2392	-2519	-5.0
<i>cis</i> -(Thiazole) <sub>2</sub> PtCl <sub>2</sub>	2.404	2.095	90.2	92.7	-1893	-1918	-1.3
<i>cis</i> -(NH <sub>3</sub> ) <sub>2</sub> Pt(CH <sub>3</sub> )Cl	2.439; 2.073	2.178; 2.286	92.8	91.7	-2006	—	—
<i>cis</i> -(NH <sub>3</sub> ) <sub>2</sub> PtBr <sub>2</sub>	2.530 <sup>e</sup>	2.164	91.0	94.5 <sup>f</sup>	-2519	-2459	2.4
<i>cis</i> -(NH <sub>3</sub> ) <sub>2</sub> PtI <sub>2</sub>	2.701 <sup>g</sup>	2.174	89.8	93.4 <sup>h</sup>	-3734	-3636	2.7
<i>cis</i> -(C <sub>5</sub> H <sub>5</sub> N) <sub>2</sub> PtI <sub>2</sub>	2.703	2.158	88.3	92.9	-3350	-3199	4.7

<sup>a</sup> In DMSO. <sup>b</sup> 1,2-DACH = R,R-cyclohexane-1,2-diamine. <sup>c</sup> 1,4-DACH = R,R-cyclohexane-1,4-diamine. <sup>d</sup> Gua = Guanine. <sup>e</sup>  $R_{\text{Pt}-\text{Br}}$ . <sup>f</sup> Br-Pt-Br bond angle. <sup>g</sup>  $R_{\text{Pt}-\text{I}}$ . <sup>h</sup> I-Pt-I bond angle.

the conformational preferences of the *cis*-(amine)<sub>2</sub>PtCl<sub>2</sub> due to steric hindrance effects strongly affect the calculated  $\delta^{(195)\text{Pt}}$  chemical shifts.

It is worth noting that previous attempts to study some correlations between  $\delta_{\text{expt}}^{(195)\text{Pt}}$  and the pK<sub>a</sub> of the amine ligands in *cis*-(amine)<sub>2</sub>PtI<sub>2</sub> complexes were based on insufficient data (only four amines were considered, namely MeNH<sub>2</sub>, EtNH<sub>2</sub>, Me<sub>2</sub>NH<sub>2</sub> and 1-adamantamine).<sup>98</sup> According to the authors these data are sufficient to show that besides the basicity of the amine, other factors like steric hindrance or solvent effects could affect the chemical shifts of the platinum complexes.

## 6. Judging the performance of the GIAO-PBE0/SARC-ZORA(Pt)U6-31+G(d)(E) computational protocol for the prediction of $^{195}\text{Pt}$ NMR chemical shifts of Pt(II) anticancer agents bearing carboxylato-leaving ligands

The performance of the GIAO-PBE0/SARC-ZORA(Pt)U6-31+G(d)(E) computational protocol was also judged in the evaluation of the  $^{195}\text{Pt}$  NMR chemical shifts of a subset (in total 8 complexes) of *cis*-bis(amine) Pt(II) anticancer agents with carboxylato-leaving ligands. Calculations of the  $^{195}\text{Pt}$  NMR chemical shifts of the carboxylato-complexes were performed in aqueous and DMF solutions employing the PCM solvation

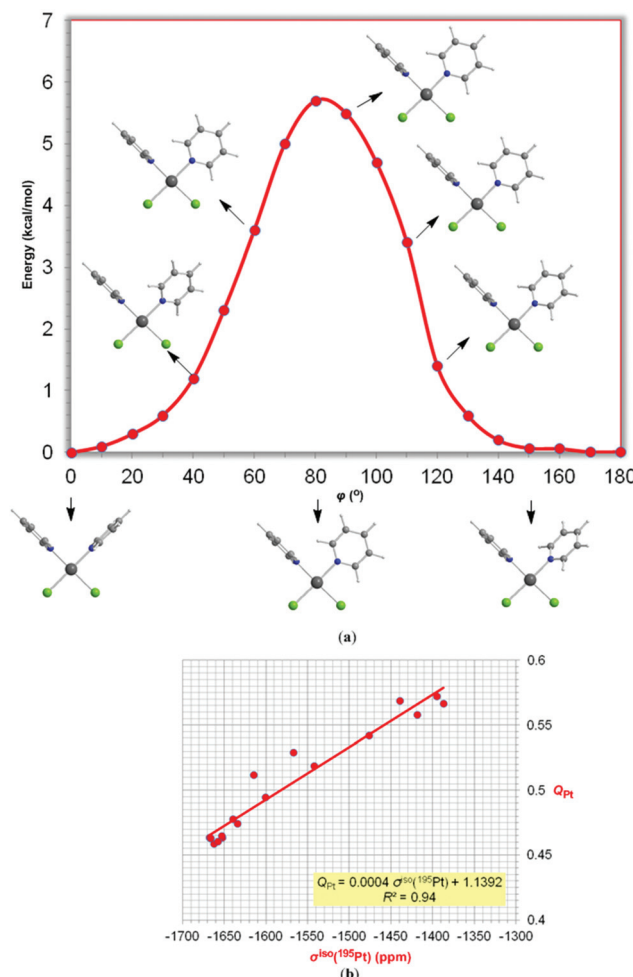


**Fig. 2** (a) Geometric and energetic profile for the diabatic rotation around the Pt–N bond of a representative *cis*-(C<sub>5</sub>H<sub>5</sub>N)<sub>2</sub>PtCl<sub>2</sub> anticancer agent and (b) the linear plot of the natural atomic charge on the Pt atom, Q<sub>pt</sub> vs. the calculated σ<sup>iso</sup>(<sup>195</sup>Pt) computed at the PBE0/SARC-ZORA(Pt)U6-31+G(d)(E) level.

model and the universal continuum solvation model based on solute electron density called SMD.<sup>53</sup> Selected structural parameters of the optimized geometries of the carboxylato-*cis*-bis(amine) Pt(II) anticancer agents are given in ESI (Table S3†), while the calculated <sup>195</sup>Pt NMR chemical shifts are compiled in Table 4.

As expected, solvation of the complexes causes elongation of the Pt–N and Pt–O bonds by 0.10–0.12 Å and 0.05–0.08 Å, respectively, in comparison with the available experimentally determined X-ray structures of carboplatin<sup>99</sup> and oxaliplatin.<sup>100</sup> On the other hand, the N–Pt–N and Cl–Pt–Cl bond angles are slightly affected by solvation. Interestingly the elongation of the Pt–O bonds is higher in aqueous than in DMF solutions, while the opposite is true for the elongation of the Pt–N bonds. It is noteworthy that the solvation model employed affects also slightly the Pt–N and Pt–O bond lengths of the complexes (the changes observed are found to be in the range of 0.002 to 0.013 Å).

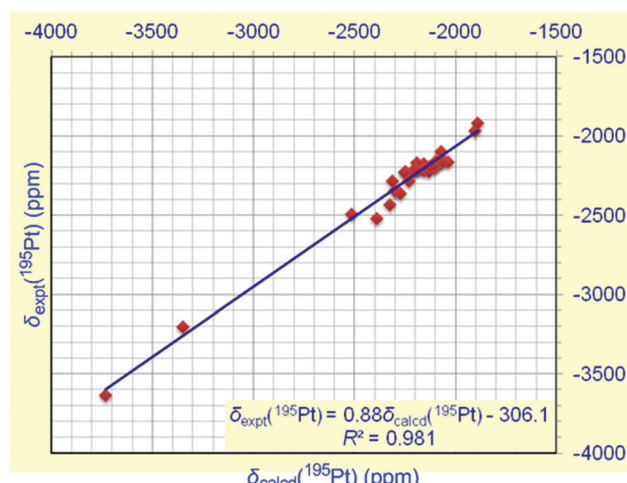


**Fig. 3** Experimental δ<sub>expt</sub>(<sup>195</sup>Pt) (ppm) vs. calculated δ<sub>calcd</sub>(<sup>195</sup>Pt) (ppm) vs. chemical shifts for *cis*-(amine)<sub>2</sub>PtX<sub>2</sub> (X = Cl, Br, I) anticancer agents. δ<sub>calcd</sub>(<sup>195</sup>Pt) (ppm) chemical shifts were computed at the GIAO-PBE0/SARC-ZORA(Pt)U6-31+G(d)(E)//PBE0/SARC-ZORA(Pt)U6-31+G(d)(E) level in DMF solutions.

An inspection of the calculated δ<sub>calcd</sub>(<sup>195</sup>Pt) and experimental δ<sub>expt</sub>(<sup>195</sup>Pt) chemical shifts given in Table 4 reveals the excellent performance of the GIAO-PBE0/SARC-ZORA(Pt)U6-31+G(d)(E) computational protocol for the calculation of δ<sup>195</sup>Pt chemical shifts in aqueous solutions employing the SMD solvation model (the mean absolute percentage deviation of the calculated from the experimental values is around 1.7%). It should be noticed that the δ<sub>expt</sub> <sup>195</sup>Pt chemical shifts in aqueous solutions where they are not available were estimated to be about 50 ppm lower from the δ<sub>expt</sub> <sup>195</sup>Pt chemical shifts in DMF solutions.<sup>101</sup> The GIAO-PBE0/SARC-ZORA(Pt)U6-31+G(d)(E) computational protocol is not a good performer for the calculation of δ<sup>195</sup>Pt chemical shifts in DMF solutions employing both the PCM and the SMD solvation models (the mean absolute percentage deviation of the calculated from the experimental values in most cases is over 10.0%). Therefore, we suggest the GIAO-PBE0/SARC-ZORA(Pt)U6-31+G(d)(E) computational protocol in combination with the SMD solvation model for the calculation of δ<sup>195</sup>Pt chemical shifts of *cis*-bis(amine) Pt(II) anticancer agents with carboxylato-leaving ligands in aqueous solutions.

The excellent performance of the GIAO-PBE0/SARC-ZORA(Pt)U6-31+G(d)(E) computational protocol in combination with the SMD solvation model in the calculation of the δ(<sup>195</sup>Pt) chemical shifts in aqueous solutions is also mirrored on the plot of δ<sub>expt</sub>(<sup>195</sup>Pt) vs. δ<sub>calcd</sub>(<sup>195</sup>Pt) chemical shifts of the *cis*-bis(amine) Pt(II) anticancer agents with carboxylato-leaving ligands shown in Fig. 6.

The plot of δ<sub>expt</sub>(<sup>195</sup>Pt) vs. δ<sub>calcd</sub>(<sup>195</sup>Pt) chemical shifts illustrates further the excellent agreement of the calculated with the experimental values. The calculated values are typically 100% of the experimental ones (setting the intercept to zero the linear relationship is δ<sub>expt</sub>(<sup>195</sup>Pt) = 1.00δ<sub>calcd</sub>(<sup>195</sup>Pt) with R<sup>2</sup> = 0.942).

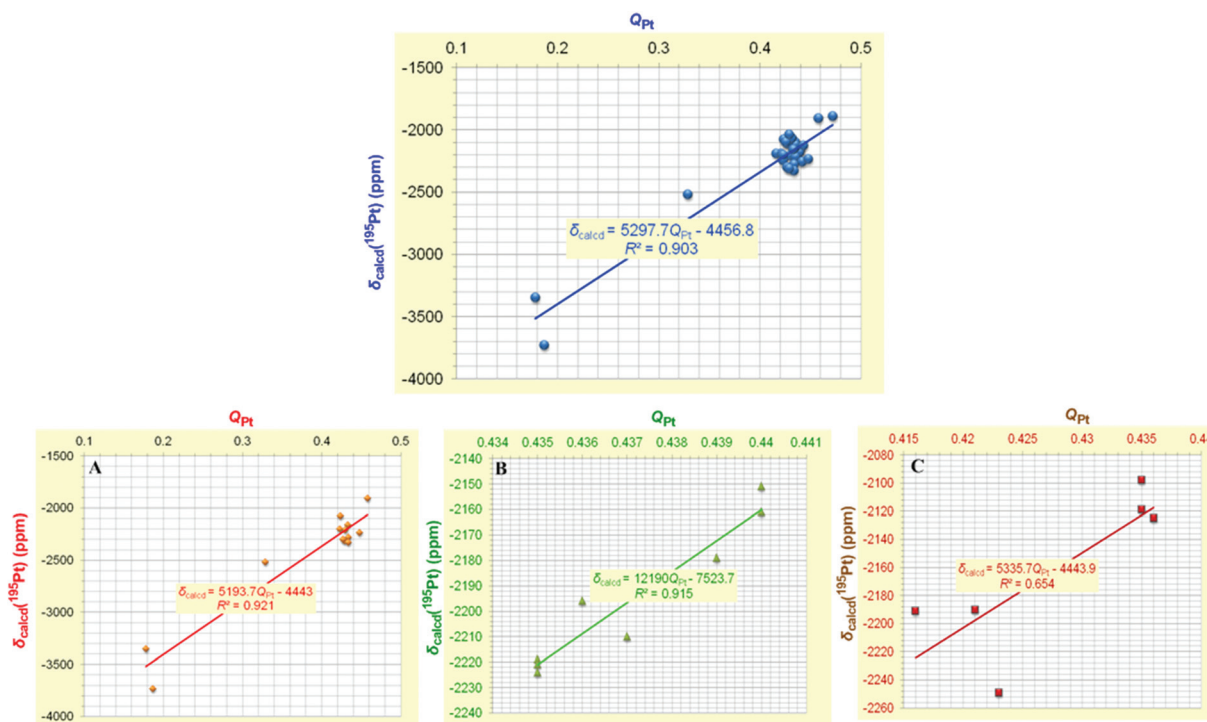


**Fig. 4** Plots of the calculated  $\delta_{\text{calcd}}(^{195}\text{Pt})$  (ppm) chemical shifts vs. the natural atomic charge  $Q_{\text{Pt}}$  for the set of *cis*-(amine)<sub>2</sub>PtX<sub>2</sub> (X = Cl, Br, I) anti-cancer agents under study along with the analogous plots for subsets of related series of *cis*-(amine)<sub>2</sub>PtX<sub>2</sub> (X = Cl, Br, I) anticancer agents exhibiting analogous steric hindrance effects.

**Table 3**  $\delta_{\text{calcd}}(^{195}\text{Pt})$  chemical shifts along with the  $(\text{p}K_a)_w$  and  $(\text{p}K_a)_{\text{AN}}$  values for the amines in a few *cis*-(amine)<sub>2</sub>PtCl<sub>2</sub> complexes

Complex	$\delta_{\text{calcd}}(^{195}\text{Pt})$ (ppm)	Amine	$(\text{p}K_a)_w$ <sup>a</sup>	$(\text{p}K_a)_{\text{AN}}$ <sup>b</sup>
<i>cis</i> -(NH <sub>3</sub> ) <sub>2</sub> PtCl <sub>2</sub>	-2076	NH <sub>3</sub>	9.21	16.46
<i>cis</i> -(CH <sub>3</sub> NH <sub>2</sub> ) <sub>2</sub> PtCl <sub>2</sub>	-2210	CH <sub>3</sub> NH <sub>2</sub>	10.62	18.37
<i>cis</i> -(C <sub>2</sub> H <sub>5</sub> NH <sub>2</sub> ) <sub>2</sub> PtCl <sub>2</sub>	-2196	C <sub>2</sub> H <sub>5</sub> NH <sub>2</sub>	10.63	18.40
<i>cis</i> -(n-C <sub>3</sub> H <sub>7</sub> NH <sub>2</sub> ) <sub>2</sub> PtCl <sub>2</sub>	-2219	n-C <sub>3</sub> H <sub>7</sub> NH <sub>2</sub>	10.53	18.22
<i>cis</i> -(n-C <sub>4</sub> H <sub>9</sub> NH <sub>2</sub> ) <sub>2</sub> PtCl <sub>2</sub>	-2224	n-C <sub>4</sub> H <sub>9</sub> NH <sub>2</sub>	10.59	18.26
<i>cis</i> -(i-C <sub>4</sub> H <sub>9</sub> NH <sub>2</sub> ) <sub>2</sub> PtCl <sub>2</sub>	-2140	i-C <sub>4</sub> H <sub>9</sub> NH <sub>2</sub>	10.43	17.92
<i>cis</i> -(C <sub>5</sub> H <sub>5</sub> N) <sub>2</sub> PtCl <sub>2</sub>	-1907	C <sub>5</sub> H <sub>5</sub> N	5.17	12.33
<i>cis</i> -(C <sub>5</sub> H <sub>10</sub> NH) <sub>2</sub> PtCl <sub>2</sub>	-2234	C <sub>5</sub> H <sub>10</sub> NH	11.22	18.92
<i>cis</i> [(CH <sub>3</sub> ) <sub>2</sub> NH] <sub>2</sub> PtCl <sub>2</sub>	-2128	C <sub>5</sub> H <sub>10</sub> NH	10.64	18.73

<sup>a</sup> In aqueous solution. <sup>b</sup> In acetonitrile solution.

## 7. Accurate prediction of $^{195}\text{Pt}$ NMR chemical shifts of *cis*-diacetyl bis(amine)platinum(II) complexes by the GIAO-PBE0/SARC-ZORA(Pt)U6-31+G(d)(E) computational protocol

We further assessed the performance of the GIAO-PBE0/SARC-ZORA(Pt)U6-31+G(d)(E) computational protocol by calculating the  $^{195}\text{Pt}$  NMR chemical shifts for a series of *cis*-diacetyl bis(amine)platinum(II) complexes (in total 12) reported recently<sup>102</sup> for which accurate experimental  $^{195}\text{Pt}$  NMR chemical shifts are available aiming to verify its broader applicability. Calculations of the  $^{195}\text{Pt}$  chemical shifts of the *cis*-diacetyl bis(amine)platinum(II) complexes were performed in solutions employing

both the PCM and SMD solvation models. Selected structural parameters of the optimized geometries of the *cis*-diacetyl bis(amine)platinum(II) complexes are given in ESI (Table S4†), while the  $^{195}\text{Pt}$  NMR chemical shifts calculated at the GIAO-PBE0/SARC-ZORA(Pt)U6-31+G(d)(E) level are compiled in Table 5.

The estimated Pt–C and Pt–N bond distances (Table S4†) were found to be in the range 2.054–2.090 and 2.299–2.396 Å, respectively. As expected, solvation of the *cis*-diacetyl bis(amine)platinum(II) complexes causes elongation of the Pt–C and Pt–N bonds by 0.09 and 0.14 Å respectively in comparison with the available experimentally determined X-ray structures.<sup>102</sup>

An inspection of the calculated  $\delta_{\text{calcd}}(^{195}\text{Pt})$  and experimental  $\delta_{\text{expt}}(^{195}\text{Pt})$  chemical shifts given in Table 5 reveals the excellent performance of the GIAO-PBE0/SARC-ZORA(Pt)U6-31+G(d)(E) computational protocol for the calculation of  $\delta$   $^{195}\text{Pt}$  chemical shifts particularly employing the PCM solvation model (the mean absolute percentage deviation of the calculated from the experimental values is around 0.9–6.0%). Note that the mean absolute percentage deviation of the calculated from the experimental values employing the SMD solvation model is around 1.5–10.3%. *The good performance of the GIAO-PBE0/SARC-ZORA(Pt)U6-31+G(d)(E) computational protocol in the prediction of  $\delta$   $^{195}\text{Pt}$  chemical shifts of the *cis*-diacetyl bis(amine)platinum(II) complexes broadens its applicability to a wider range of square planar Pt(II) complexes.*

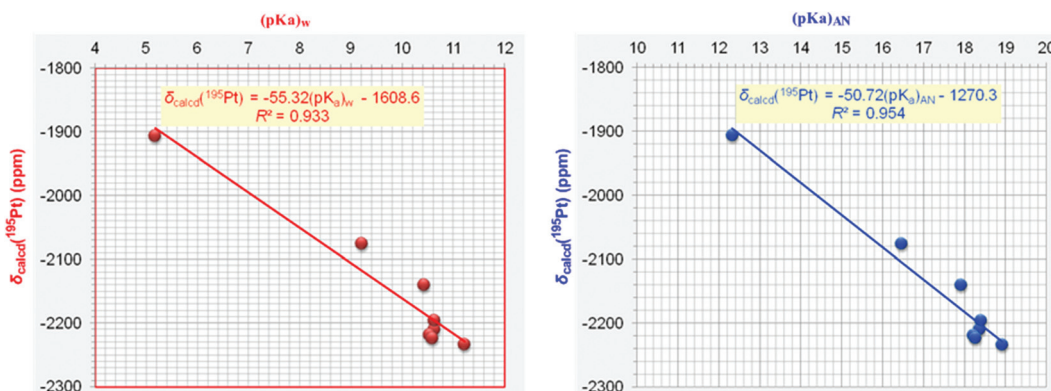


**Fig. 5** Calculated  $\delta_{\text{calcd}}^{195}\text{Pt}$  (ppm) vs.  $(\text{p}K_a)_w$  and  $(\text{p}K_a)_{\text{AN}}$  of the protonated amines for eight *cis*-(amine)<sub>2</sub>PtCl<sub>2</sub> anticancer agents for which experimental  $\text{p}K_a$  values are available.

**Table 4**  $^{195}\text{Pt}$  NMR chemical shifts (in ppm) for *cis*-bis(amine) Pt(II) anticancer agents with carboxylato-leaving ligands referenced to  $[\text{PtCl}_4]^{2-}$  ( $\delta_{\text{ref}}^{\text{iso}} = -3294$  ppm) calculated at the GIAO-PBE0/SARC-ZORA(Pt)U6-31+G(d)(E) level in solution employing the PCM and SMD solvation models

Compound	$\delta_{\text{theor}}^{195}\text{Pt}$		$\delta_{\text{expt}}^{195}\text{Pt}$	Solvent	Dev. (%)	
	PCM	SMD			PCM	SMD
Carboplatin <sup>a</sup>	-1464 -1687	-1990 -1763	-1723 (-1755) <sup>b</sup>	DMF Water <sup>c</sup>	-15.0 -4.9	21.5 <b>0.5</b>
Oxaliplatin <sup>a</sup>	-1710	-2361	-1989 (-2039)	DMF Water	-4.4 -2.4	32.0 <b>2.1</b>
<i>cis</i> -(NH <sub>3</sub> ) <sub>2</sub> Pt(OOCCH <sub>3</sub> ) <sub>2</sub>	-1111 -1150	-1698 -1594	-1565 -1615	DMF Water	-29.0 -28.8	8.5 <b>-1.3</b>
<i>cis</i> -(NH <sub>3</sub> ) <sub>2</sub> Pt(OOCC <sub>6</sub> H <sub>5</sub> ) <sub>2</sub>	-1092	-1682	-1552 (-1602)	DMF Water	-29.6 -1.4	8.4
(C <sub>5</sub> H <sub>10</sub> NH) <sub>2</sub> Pt(OOCCOO)	-1592 -1815	-2177 -1870	-1995 (-1945)	DMF Water	-19.5 -10.5	10.1 <b>-3.9</b>
(1,4-DACH)Pt(OOCCOO)	-1617	-2193	(-1781)	DMF	-9.2	23.1
(1,4-DACH)Pt(CBDCA) <sup>e</sup>	-1646 -1616	-1862 -2103	-1831 (-1809)	Water DMF	-10.1 -10.7	1.7 16.3
(1,4-DACH)Pt(OOCCH <sub>2</sub> COO)	-1630 -1859	-2130 -1898	(-1809) -1859	DMF Water	-9.9 0.0	17.7 <b>2.1</b>

<sup>a</sup> Carboplatin = *cis*-diamine(1,1-cyclobutanedicarboxylato)platinum(II). <sup>b</sup> The  $\delta_{\text{expt}}^{195}\text{Pt}$  chemical shifts in aqueous solutions where they are not available were estimated to be about 50 ppm lower from the  $\delta_{\text{expt}}^{195}\text{Pt}$  chemical shifts in DMF solutions (figures in parentheses). <sup>c</sup> Employing the Gaussian03 package for calculations in aqueous solution using the PCM model. <sup>d</sup> Oxaliplatin = (DACH)(oxalato)platinum(II). <sup>e</sup> CBDCA = 1,1-cyclobutanedicarboxylate.

## 8. Extending the applicability of the GIAO-PBE0/SARC-ZORA(Pt)U6-31+G(d)(E) computational protocol in the prediction of $^{195}\text{Pt}$ NMR chemical shifts of octahedral Pt(IV) anticancer agents

The performance of the GIAO-PBE0/SARC-ZORA(Pt)U6-31+G(d)(E) computational protocol was also judged in the evaluation of the  $^{195}\text{Pt}$  NMR chemical shifts of a subset of octahedral Pt(IV) anticancer agents (in total 20) for which experimental data are available.

Calculations of the  $^{195}\text{Pt}$  NMR chemical shifts of the octahedral Pt(IV) anticancer agents were performed in solutions employing both the PCM and SMD solvation models. Selected structural parameters of the optimized geometries of the octahedral Pt(IV) anticancer agents are given in ESI (Table S5†).

while the  $^{195}\text{Pt}$  NMR chemical shifts calculated at the GIAO-PBE0/SARC-ZORA(Pt)U6-31+G(d)(E) level are compiled in Table 6.

Perusal of Table S5† illustrates the strong solvent effects on the structural parameters of the octahedral Pt(IV) complexes studied, which are also affected by the solvation model employed. As expected, solvation of the complexes, independently of the solvent used, causes elongation of the Pt–O, Pt–Cl and Pt–N bonds by 0.03–0.06 Å, 0.04–0.06 Å and 0.05–0.11 Å respectively in comparison with the available experimentally determined X-ray structures of the *cct*-[PtCl<sub>2</sub>(NH<sub>3</sub>)(C<sub>6</sub>H<sub>11</sub>NH<sub>2</sub>)(OCOCH<sub>3</sub>)<sub>2</sub>]<sup>114</sup> *cct*-[PtCl<sub>2</sub>(NH<sub>3</sub>)<sub>2</sub>(OCOCH<sub>3</sub>)<sub>2</sub>]<sup>115</sup> *cct*-[PtCl<sub>2</sub>(1,2-DACH)<sub>2</sub>(OCOCH<sub>3</sub>)<sub>2</sub>]<sup>109</sup> *cct*-[PtCl<sub>2</sub>(1,4-DACH)<sub>2</sub>(OCOCH<sub>3</sub>)<sub>2</sub>]<sup>108</sup> *cct*-[PtCl<sub>2</sub>(NH<sub>3</sub>)<sub>2</sub>(OCONHR<sub>3</sub>)<sub>2</sub>] (R = <sup>3</sup>Bu, *c*-pentyl, *c*-hexyl, phenyl),<sup>104</sup> and *cct*-[PtCl<sub>2</sub>(NH<sub>3</sub>)<sub>2</sub>(OH)<sub>2</sub>]<sup>116</sup> complexes. The O-

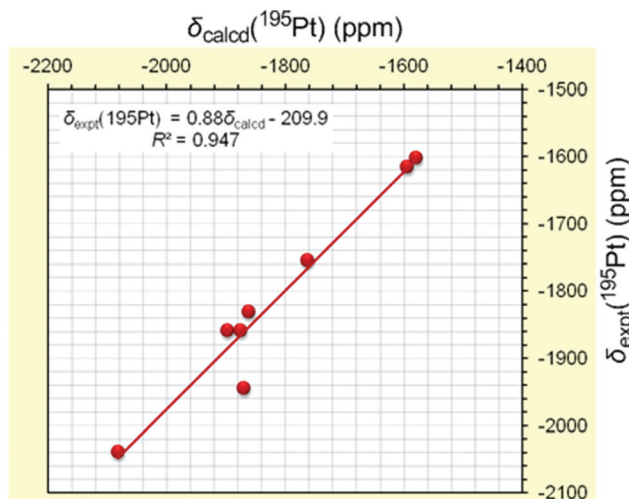


**Fig. 6**  $\delta_{\text{expt}}(^{195}\text{Pt})$  (ppm) vs.  $\delta_{\text{calcd}}(^{195}\text{Pt})$  (ppm) chemical shifts for *cis*-bis-(amine) Pt(II) anticancer agents with carboxylato-leaving ligands.  $\delta_{\text{calcd}}(^{195}\text{Pt})$  (ppm) chemical shifts were computed at the GIAO-PBE0/SARC-ZORA(Pt)U6-31+G(d)(E) level in aqueous solution employing the SMD solvation model.

Pt–O, Cl–Pt–Cl and N–Pt–N bond angles are slightly affected by solvation; the changes observed amount to 1–5, 1–6 and 0.2–3° respectively. The observed solvent effects on the structural parameters of the complexes probably overcome the relativistic effects, and therefore the successful applicability of the non-relativistic GIAO-PBE0/SARC-ZORA(Pt)U6-31+G(d)(E) computational protocol in producing reliable  $\delta_{\text{calcd}}(^{195}\text{Pt})$  chemical shifts could be understood.

Inspection of Table 6 reveals the excellent performance of the GIAO-PBE0/SARC-ZORA(Pt)U6-31+G(d)(E) computational protocol for the calculation of  $\delta(^{195}\text{Pt})$  chemical shifts of the octahedral Pt(IV) complexes involving carboxylato- and carbamato-leaving groups, particularly employing the PCM solvation model (the mean absolute percentage deviation of the calculated from the experimental values is around 0.5–9.9%).

**Table 5**  $^{195}\text{Pt}$  NMR chemical shifts (in ppm) for a series of *cis*-diacetyl bis(amine)platinum(IV) complexes referenced to  $[\text{PtCl}_6]^{2-}$ ,<sup>a</sup> calculated at the GIAO-PBE0/SARC-ZORA(Pt)U6-31+G(d)(E) level in solution

Compound	$\delta_{\text{theor}}(^{195}\text{Pt})$		$\delta_{\text{expt}}(^{195}\text{Pt})^b$	Solvent	Dev. (%)	
	PCM	SMD			PCM	SMD
<i>cis</i> -Pt(OCMe) <sub>2</sub> (H <sub>2</sub> NET) <sub>2</sub>	-3458	-3595	-3274	CHCl <sub>3</sub>	5.6	9.8
<i>cis</i> -Pt(OCMe) <sub>2</sub> (H <sub>2</sub> NPr) <sub>2</sub>	-3405	-3543	-3304	CHCl <sub>3</sub>	3.1	7.2
<i>cis</i> -Pt(OCMe) <sub>2</sub> (H <sub>2</sub> NCH <sub>2</sub> Ph) <sub>2</sub>	-3481	-3608	-3329	CHCl <sub>3</sub>	4.6	8.4
<i>cis</i> -Pt(OCMe) <sub>2</sub> (H <sub>2</sub> NCH <sub>2</sub> CH <sub>2</sub> Ph) <sub>2</sub>	-3466	-3602	-3299	CHCl <sub>3</sub>	5.1	9.2
<i>cis</i> -Pt(OCMe) <sub>2</sub> (H <sub>2</sub> NCH <sub>2</sub> CH=CH <sub>2</sub> )	-3468	-3608	-3272	CHCl <sub>3</sub>	6.0	10.3
<i>cis</i> -Pt(OCMe) <sub>2</sub> (H <sub>2</sub> NCy) <sub>2</sub>	-3484	-3521	-3296	CHCl <sub>3</sub>	2.7	6.8
<i>cis</i> -Pt(OCMe) <sub>2</sub> (HNMe) <sub>2</sub>	-3406	-3572	-3439	CH <sub>2</sub> Cl <sub>2</sub>	-1.0	3.9
<i>cis</i> -Pt(OCMe) <sub>2</sub> (HNET) <sub>2</sub>	-3368	-3525	-3399	CH <sub>2</sub> Cl <sub>2</sub>	-0.9	3.7
<i>cis</i> -Pt(OCMe) <sub>2</sub> (H <sub>2</sub> NCH <sub>2</sub> CH <sub>2</sub> NH <sub>2</sub> )	-3379	-3507	-3337	CHCl <sub>3</sub>	1.3	5.1
<i>cis</i> -Pt(OCMe) <sub>2</sub> (Me <sub>2</sub> NCH <sub>2</sub> CH <sub>2</sub> NH <sub>2</sub> )	-3428	-3509	-3347	CHCl <sub>3</sub>	2.4	4.8
<i>cis</i> -Pt(OCMe) <sub>2</sub> (MeNHCH <sub>2</sub> CH <sub>2</sub> NHMe)	-3421	-3550	-3293	CHCl <sub>3</sub>	3.9	7.8
<i>cis</i> -Pt(OCMe) <sub>2</sub> (Me <sub>2</sub> NCH <sub>2</sub> CH <sub>2</sub> NMe <sub>2</sub> )	-3319	-3481	-3430	CH <sub>2</sub> Cl <sub>2</sub>	-3.2	-1.5

<sup>a</sup> Calculated  $\sigma(^{195}\text{Pt})$  ( $[\text{PtCl}_6]^{2-}$ ) values of -1600 and -1680 ppm employing the PCM and SMD solvation models respectively. <sup>b</sup> Ref. 102.

For the dihydroxo Pt(IV) complexes the performance of the GIAO-PBE0/SARC-ZORA(Pt)U6-31+G(d)(E) computational protocol seems to be no good (the mean absolute percentage deviation of the calculated from the experimental values is around 21–31%). The performance becomes better when the 6-31G(d,p) basis set for the non-metal elements is used (in this case the mean absolute percentage deviation of the calculated from the experimental values is around 9–18%). We believe that the higher deviations of the calculated from the experimental values of  $\delta(^{195}\text{Pt})$  chemical shifts of the dihydroxo Pt(IV) complexes could be due to the fact that the experimental assignments refer to a different composition of the dihydroxo complexes in solutions than that used in the calculations, and different hydrogen bonding and dimeric species. Probably better agreement with the theoretical data can be achieved by reassigning some of the experimental shielding constants.

The excellent performance of the GIAO-PBE0/SARC-ZORA(Pt)U6-31+G(d)(E) and GIAO-PBE0/SARC-ZORA(Pt)U6-31G(d,p)(E) computational protocols in combination with the PCM solvation model in the calculation of the  $\delta(^{195}\text{Pt})$  chemical shifts in solutions of the octahedral Pt(IV) anticancer agents is mirrored on the plot of  $\delta_{\text{expt}}(^{195}\text{Pt})$  vs.  $\delta_{\text{calcd}}(^{195}\text{Pt})$  chemical shifts shown in Fig. 7.

The plot of  $\delta_{\text{expt}}(^{195}\text{Pt})$  vs.  $\delta_{\text{calcd}}(^{195}\text{Pt})$  chemical shifts illustrates further the excellent agreement of the calculated with the experimental values. The calculated values are typically 94% of the experimental ones (setting intercept to zero, the linear relationship is  $\delta_{\text{calcd}}(^{195}\text{Pt}) = 0.942\delta_{\text{expt}}(^{195}\text{Pt})$  with a  $R^2 = 0.897$ ).

## Conclusions

The successful computation of accurate  $^{195}\text{Pt}$  chemical shifts for a series of *cis*-(amine)<sub>2</sub>PtX<sub>2</sub> (X = Cl, Br, I), *cis*-bis(amine) Pt(II) anticancer agents with carboxylato- or acetoxy-leaving ligands as well as octahedral Pt(IV) anticancer agents was achieved employing the GIAO-PBE0/SARC-ZORA(Pt)U6-31+G(d)(E)

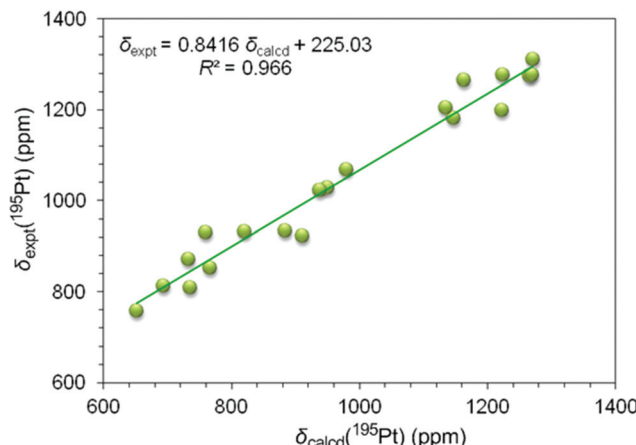


**Fig. 7**  $\delta_{\text{expt}}(^{195}\text{Pt})$  (ppm) vs.  $\delta_{\text{calcd}}(^{195}\text{Pt})$  (ppm) chemical shifts for octahedral Pt(iv) anticancer agents.  $\delta_{\text{calcd}}(^{195}\text{Pt})$  (ppm) chemical shifts were computed at the GIAO-PBE0/SARC-ZORA(Pt)U6-31+G(d)(E) level in solution employing the PCM solvation model.

computational protocol. Important results are summarized as follows:

1.  $^{195}\text{Pt}$  NMR chemical shifts of a wide range of square planar Pt(II) and octahedral Pt(IV) complexes have been computed with the GIAO DFT method employing in total 25 DFs. The benchmark calculations showed that the GIAO-PBE0/SARC-ZORA(Pt)U6-31+G(d)(E) computational protocol provides the most accurate predictions of the  $^{195}\text{Pt}$  chemical shifts for these complexes.

2. The GIAO-PBE0/SARC-ZORA(Pt)U6-31+G(d)(E) computational protocol is offered for the accurate prediction of the  $^{195}\text{Pt}$  NMR chemical shifts of a series of *cis*-(amine)<sub>2</sub>PtX<sub>2</sub> (X = Cl, Br, I) anticancer agents (in total 42 complexes) in solutions employing the Polarizable Continuum Model (PCM) solvation model.

3. Calculations of the torsional energy curves along the diabatic (unrelaxed) rotation around the Pt–N bond of the *cis*-(amine)<sub>2</sub>PtX<sub>2</sub> (X = Cl, Br, I) anticancer agents revealed the high sensitivity of the  $^{195}\text{Pt}$  NMR chemical shifts to conformational changes induced by the free rotation of the amine ligands around the Pt–N bond of the anticancer agents.

**Table 6**  $^{195}\text{Pt}$  NMR chemical shifts (in ppm) for selected octahedral Pt(IV) anticancer agents referenced to  $[\text{PtCl}_6]^{2-}$ ,<sup>a</sup> calculated at the GIAO-PBE0/SARC-ZORA(Pt)U6-31+G(d)(E) level in solution

Compound	$\delta_{\text{theor}}(^{195}\text{Pt})$		$\delta_{\text{expt}}(^{195}\text{Pt})$	Solvent	Dev. (%)	
	PCM	SMD			PCM	SMD
<i>cct</i> -[Pt(NH <sub>3</sub> ) <sub>2</sub> Cl <sub>2</sub> (OOCH) <sub>2</sub> ]	980	925	1068 <sup>b</sup>	DMSO	-8.2	-13.4
<i>cct</i> -[Pt(NH <sub>3</sub> ) <sub>2</sub> Cl <sub>2</sub> (OOCCH <sub>3</sub> ) <sub>2</sub> ] (Satraplatin)	1222	1181	1198 <sup>c</sup>	Water	2.0	-1.4
<i>cct</i> -[Pt(NH <sub>3</sub> ) <sub>2</sub> Cl <sub>2</sub> (OOCCH <sub>3</sub> ) <sub>2</sub> ] <sup>d</sup>	1141	1147		Water		
<i>cct</i> -[Pt(NH <sub>3</sub> ) <sub>2</sub> Cl <sub>2</sub> (OOCF) <sub>2</sub> ] <sup>e</sup>	1147	1177	1182 <sup>e</sup>	Water	-3.0	-0.4
<i>cct</i> -[Pt(NH <sub>3</sub> ) <sub>2</sub> Cl <sub>2</sub> (OOCCHCl <sub>2</sub> ) <sub>2</sub> ] (Mitaplatin)	1134	1070	1205 <sup>f</sup>	DMSO	-5.9	-11.2
Pt(en)Cl <sub>2</sub> (OOCCH <sub>3</sub> ) <sub>2</sub>	950	892	1028 <sup>g</sup>	DMSO	-7.6	-13.2
Pt(en)Cl <sub>2</sub> (OOCF <sub>3</sub> ) <sub>2</sub>	883	956	934 <sup>g</sup>	Water	-5.5	2.4
	910	958	923 <sup>g</sup>	MeOH	-1.4	3.8
<i>cct</i> -Pt(1,2-DACH)Cl <sub>2</sub> (OOCCH <sub>3</sub> ) <sub>2</sub>	937	882	1022 <sup>h</sup>	Acetone	-8.3	-13.7
<i>cct</i> -Pt(1,4-DACH)Cl <sub>2</sub> (OOCCH <sub>3</sub> ) <sub>2</sub>	1218	1199	1108 <sup>i</sup>	Acetone	9.9	8.2
<i>cct</i> -{Pt(NH <sub>3</sub> ) <sub>2</sub> Cl <sub>2</sub> [OOCNH( <sup>t</sup> Bu)] <sub>2</sub> }	1224	1154	1276 <sup>e</sup>	DMSO	-4.1	-9.6
<i>cct</i> -{Pt(NH <sub>3</sub> ) <sub>2</sub> Cl <sub>2</sub> [OOCNH( <i>c</i> -pentyl)] <sub>2</sub> }	1266	1182	1274 <sup>e</sup>	DMSO	-0.6	-7.2
<i>cct</i> -{Pt(NH <sub>3</sub> ) <sub>2</sub> Cl <sub>2</sub> [OOCNH( <i>c</i> -hexyl)] <sub>2</sub> }	1269	1231	1276 <sup>e</sup>	DMSO	-0.5	-3.5
<i>cct</i> -[Pt(NH <sub>3</sub> ) <sub>2</sub> Cl <sub>2</sub> (OOCNHPH) <sub>2</sub> ]	1163	1151	1265 <sup>e</sup>	DMSO	-8.1	-9.0
Pt(1,2-DACH)(OH) <sub>2</sub> (oxalate)	1280	1164	1310 <sup>j</sup>	DMF	-2.3	-11.1
	(1271) <sup>k</sup>	(1172)			(-3.0)	(-10.5)
<i>cct</i> -[Pt(NH <sub>3</sub> ) <sub>2</sub> Cl <sub>2</sub> (OH) <sub>2</sub> ] (Oxoplatin)	612	582	853 <sup>l</sup>	Water	-28.3	-31.8
	(766)	(702)			(-10.2)	(-17.7)
<i>cct</i> -[Pt(iPrNH <sub>2</sub> ) <sub>2</sub> Cl <sub>2</sub> (OH) <sub>2</sub> ] (Iproplatin)	678	695	932 <sup>m</sup>	Water	-27.3	-25.4
	(820)	(768)			(-12.0)	(-17.6)
Pt(hpip)Cl <sub>2</sub> (OH) <sub>2</sub>	539	550	757 <sup>n</sup>	Water	-28.8	-27.3
	(652)	(636)			(-13.9)	(-16.6)
Pt(mhpip)Cl <sub>2</sub> (OH) <sub>2</sub>	586	587	812 <sup>n</sup>	Water	-27.8	-27.8
	(694)	(677)			(-14.5)	(-16.6)
Pt(dmhpip)Cl <sub>2</sub> (OH) <sub>2</sub>	639	660	808 <sup>n</sup>	Water	-20.9	-18.3
	(735)	(725)			(-9.0)	(-10.3)
Pt(1,4-DACH)(OH) <sub>2</sub> Cl <sub>2</sub>	609	622	885 <sup>h</sup>	Water	-31.2	-29.7
	(727)	(706)			(-17.9)	(-20.2)
	614	583	872 <sup>h</sup>	DMF	-29.6	-33.1
	(732)	(707)			(-16.1)	(-18.9)

<sup>a</sup> Calculated  $\sigma^{195}\text{Pt}$  ( $[\text{PtCl}_6]^{2-}$ ) values in the various solvents employing the PCM and SMD solvation models (cf. Table 1). <sup>b</sup> Ref 103. <sup>c</sup> Ref. 92. <sup>d</sup> No experimental data available. <sup>e</sup> Ref. 104. <sup>f</sup> Ref. 105. <sup>g</sup> Ref. 106. <sup>h</sup> Ref. 107. <sup>i</sup> Ref. 108. <sup>j</sup> Ref. 110. <sup>k</sup> Figures in parentheses are  $\delta_{\text{calcd}}(^{195}\text{Pt})$  NMR chemical shifts using the 6-31G(d,p) basis set for the non-metal atoms. <sup>l</sup> Ref. 111. <sup>m</sup> Ref. 112. <sup>n</sup> Ref. 113.

4. The crucial role of the conformational preferences on the electron density of the Pt central atom and consequently on the calculated  $\delta^{195}\text{Pt}$  chemical shifts is mirrored on the excellent linear plots of  $\delta_{\text{calcd}}(^{195}\text{Pt})$  chemical shifts *vs.* the natural atomic charge  $Q_{\text{Pt}}$ .

5. The  $\delta_{\text{calcd}}(^{195}\text{Pt})$  chemical shifts of the *cis*-(amine)<sub>2</sub>PtX<sub>2</sub> (X = Cl, Br, I) anticancer agents was found to correlate linearly with the  $pK_a$  of the protonated amine ligands. Including in the correlations the data for the outlier *cis*-[(CH<sub>3</sub>)<sub>2</sub>NH]<sub>2</sub>PtCl<sub>2</sub> complex the linear relationships,  $\delta_{\text{calcd}}(^{195}\text{Pt}) = -53.43(pK_a)_w - 1619.6$  ( $R^2 = 0.886$ ) and  $\delta_{\text{calcd}}(^{195}\text{Pt}) = -47.43(pK_a)_{\text{AN}} - 1317.6$  ( $R^2 = 0.873$ ) were obtained. The lower  $R^2$  values indicate that the conformational preferences of the *cis*-(amine)<sub>2</sub>PtCl<sub>2</sub> due to steric hindrance effects strongly affect the calculated  $\delta(^{195}\text{Pt})$  chemical shifts.

6. The GIAO-PBE0/SARC-ZORA(Pt)U6-31+G(d)(E) computational protocol in combination with the universal continuum solvation model called the SMD model for aqueous solutions is also offered for the accurate prediction of the  $^{195}\text{Pt}$  NMR chemical shifts of the *cis*-bis(amine)Pt(II) anticancer agents bearing carboxylato- as the leaving ligands.

7. The good performance of the GIAO-PBE0/SARC-ZORA-(Pt)U6-31+G(d)(E) computational protocol in the prediction of  $\delta^{195}\text{Pt}$  chemical shifts of a series of *cis*-diacetyl bis(amine)platinum(II) complexes broadens its applicability to a wider range of square planar Pt(II) complexes. The mean absolute percentage deviation of the calculated from the experimental values is around 0.9–6.0%.

8. The GIAO-PBE0/SARC-ZORA(Pt)U6-31+G(d)(E) computational protocol also performs well for the calculation of  $\delta^{195}\text{Pt}$  chemical shifts of octahedral Pt(IV) complexes involving carboxylato- and carbamato-leaving groups, particularly employing the PCM solvation model (the mean absolute percentage deviation of the calculated from the experimental values is around 0.5–9.9%).

9. For the dihydroxo Pt(IV) complexes the performance of the GIAO-PBE0/SARC-ZORA(Pt)U6-31+G(d)(E) computational protocol seems to be no good (the mean absolute percentage deviation of the calculated from the experimental values is around 21–31%). The performance becomes better when the 6-31G(d,p) basis set for the non-metal elements is used (in this case the mean absolute percentage deviation of the calculated from the experimental values is around 9–18%). The higher deviations of the calculated from the experimental values of  $\delta^{195}\text{Pt}$  chemical shifts of the dihydroxo Pt(IV) complexes are probably due to the fact that the experimental assignments refer to a different composition of the dihydroxo complexes in solutions than that used in the calculations, and different hydrogen bonding and dimeric species.

10. The excellent performance of the computational protocol employed in the calculation of the  $\delta(^{195}\text{Pt})$  chemical shifts of square planar Pt(II) and octahedral Pt(IV) anticancer agents is mirrored on the plot of  $\delta_{\text{expt}}(^{195}\text{Pt})$  *vs.*  $\delta_{\text{calcd}}(^{195}\text{Pt})$  chemical shifts.

Considering all these results, we believe that the GIAO-PBE0/SARC-ZORA(Pt)U6-31+G(d)(E) computational

protocol for the calculation of  $^{195}\text{Pt}$  chemical shifts reported herein contributes to the difficult task of computation of  $^{195}\text{Pt}$  NMR.

## Notes and references

- J. R. L. Priqueler, I. S. Butler and F. D. Rochon, *Appl. Spectrosc. Rev.*, 2006, **41**, 185–226.
- P. S. Pregosin, *Coord. Chem. Rev.*, 1982, **44**, 247–291.
- E. Gabano, E. Marengo, M. Bobba, E. Robotti, C. Cassino, M. Botta and D. Osella, *Coord. Chem. Rev.*, 2006, **250**, 2158–2174.
- B. M. Still, P. G. Anil Kumar, J. R. Aldrich-Wright and W. S. Price, *Chem. Soc. Rev.*, 2007, **36**, 665–686.
- J. C. Facelli, *Concepts Magn. Reson.*, 2004, **20A**, 42–69.
- M. Kaupp, M. Bühl and V. G. Malkin, *Calculation of NMR and EPR Parameters: Theory and Applications*, Wiley-VCH, Weinheim, 2004.
- M. Bühl, *Annu. Rep. NMR Spectrosc.*, 2008, **64**, 77–126.
- J. Autschbach and S. Zheng, *Annu. Rep. NMR Spectrosc.*, 2009, **67**, 1–95.
- A. Pidcock, R. E. Richards and L. M. Venanzi, *J. Chem. Soc. A*, 1968, 1970–1973.
- R. R. Dean and J. C. Green, *J. Chem. Soc. A*, 1968, 3047–3050.
- V. G. Malkin, O. L. Malkina, L. A. Erickson and D. R. Salahub, in *Modern Density Functional Theory: A Tool for Chemistry*, ed. P. Politzer and J. M. Seminario, Elsevier, Amsterdam, 1995, vol. 2.
- J. Autschbach, Calculation of heavy-nucleus chemical shifts: Relativistic all-electron methods, in *Calculation of NMR and EPR Parameters. Theory and Applications*, ed. M. Kaupp, M. Bühl and V. G. Malkin, Wiley-VCH, Weinheim, 2004.
- M. Sterzel and J. Autschbach, *Inorg. Chem.*, 2006, **45**, 3316–3324.
- M. Bühl, NMR of transition metal compounds, in *Calculation of NMR and EPR Parameters. Theory and Applications*, ed. M. Kaupp, M. Bühl and V. G. Malkin, Wiley-VCH, Weinheim, 2004, pp. 421–431.
- P. Pykkö, *Theor. Chem. Acc.*, 2000, **103**, 214.
- C. Benzi, O. Crescenzi, M. Pavone and V. Barone, *Magn. Reson. Chem.*, 2004, **42**, S57.
- R. C. Mawhinney and G. Srhreckenbach, *Magn. Reson. Chem.*, 2004, **42**, S88.
- T. M. Gilbert and T. Ziegler, *J. Phys. Chem. A*, 1999, **103**, 7535–7543.
- J. Autschbach and B. L. Guennic, *Chem.-Eur. J.*, 2004, **10**, 2581–2589.
- B. L. Guennic, K. Matsumoto and J. Autschbach, *Magn. Reson. Chem.*, 2004, **42**, S99–S116.
- E. P. Fowe, P. Belser, C. Daul and H. Chermette, *Phys. Chem. Chem. Phys.*, 2005, **7**, 1732–1738.

- 22 K. R. Koch, M. R. Burger, J. Kramer and A. N. Westra, *Dalton Trans.*, 2006, 3277–3284.
- 23 S. K. Wolff, T. Ziegler, E. van Lenthe and E. J. Baerends, *J. Chem. Phys.*, 1999, **110**, 768.
- 24 J. G. Snijders, E. J. Baerends and P. Ros, *Mol. Phys.*, 1979, **38**, 1909.
- 25 L. A. Truflandier and J. Autschbach, *J. Am. Chem. Soc.*, 2010, **132**, 3472–3483.
- 26 J. Vaara, *Phys. Chem. Chem. Phys.*, 2007, **9**, 5399–5418.
- 27 M. R. Burger, J. Kramer, H. Chermette and K. R. Koch, *Magn. Reson. Chem.*, 2010, **48**, S38–S47.
- 28 L. A. Truflandier, K. Sutter and J. Autschbach, *Inorg. Chem.*, 2011, **50**, 1723–1732.
- 29 K. Sutter and J. Autschbach, *J. Am. Chem. Soc.*, 2012, **134**, 13374–13385.
- 30 C. J. Pickard and F. Mauri, *Phys. Rev. B: Condens. Matter*, 2001, **63**, 245101.
- 31 C. Bonhomme, C. Gervais, F. Babonneau, C. Coelho, F. Pourpoint, T. Azaïs, S. E. Ashbrook, J. M. Griffin, J. R. Yates, F. Mauri and C. J. Pickard, *Chem. Rev.*, 2012, **112**, 5733–5779.
- 32 B. E. G. Lucier, A. R. Reidel and R. B. Schurko, *Can. J. Chem.*, 2011, **89**, 919–937.
- 33 J. Reedijk, *J. Inorg. Biochem.*, 2003, **96**, 81.
- 34 J. Reedijk, *Proc. Natl. Acad. Sci. U. S. A.*, 2003, **100**, 3611–3616.
- 35 T. Boulikas, A. Pantos, E. Bellis and P. Christofis, *Cancer Ther.*, 2007, **5**, 537–583.
- 36 J. J. Wilson and S. J. Lippard, *Chem. Rev.*, 2013, DOI: 10.1021/cr4004314.
- 37 T. A. Connors, M. Jones, W. C. J. Ross, D. Braddock, A. R. Khokhar and M. L. Tobe, *Chem.-Biol. Interact.*, 1972, **5**, 415–424.
- 38 D. Braddock, T. A. Connors, M. Jones, W. C. J. Ross, A. R. Khokhar, D. H. Melzack and M. L. Tobe, *Chem.-Biol. Interact.*, 1975, **11**, 145–161.
- 39 M. J. Cleare and J. D. Hoeschele, *Bioinorg. Chem.*, 1973, **2**, 187–210.
- 40 M. J. Cleare and J. D. Hoeschele, *Platinum Metals Rev.*, 1973, **17**, 2–13.
- 41 P. G. Abdoul-Ahad and G. A. Webb, *Int. J. Quantum Chem.*, 1982, **XXI**, 1105–1115.
- 42 P. Gramatica, E. Papa, M. Luini, E. Monti, M. B. Garibaldi, M. Ravera, E. Gabano, L. Gaviglio and D. Osella, *J. Biol. Inorg. Chem.*, 2010, **15**, 1157–1169.
- 43 M. J. Frisch, et al. *Gaussian 09, Revision B.01*, Gaussian, Inc., Wallingford CT, 2010. See Electronic Supporting Information for the full reference.
- 44 M. Ernzerhof and G. E. Scuseria, *J. Chem. Phys.*, 1999, **110**, 5029.
- 45 C. Adamo and V. Barone, *Chem. Phys. Lett.*, 1997, **274**, 242.
- 46 C. Adamo and V. Barone, *J. Chem. Phys.*, 1999, **110**, 6160.
- 47 C. Adamo, G. E. Scuseria and V. Barone, *J. Chem. Phys.*, 1999, **111**, 2889.
- 48 C. Adamo and V. Barone, *Theor. Chem. Acc.*, 2000, **105**, 169.
- 49 V. Veter, C. Adamo and P. Maldivi, *Chem. Phys. Lett.*, 2000, **325**, 99.
- 50 D. A. Pantazis, X.-Y. Chen, C. R. Landis and F. Neese, *J. Chem. Theor. Comput.*, 2008, **4**, 908.
- 51 EMSL basis set exchange, <https://bse.pnl.gov/bse/portal>, accessed 08-01-2013.
- 52 J. Tomasi, B. Mennucci and R. Cammi, *Chem. Rev.*, 2005, **105**, 2999–3093.
- 53 A. V. Marenich, C. J. Cramer and D. G. Truhlar, *J. Phys. Chem. B*, 2009, **113**, 6378–6396.
- 54 R. Ditchfield, *Mol. Phys.*, 1974, **27**, 789.
- 55 J. Gauss, *J. Chem. Phys.*, 1993, **99**, 3629.
- 56 J. C. Slater, *Phys. Rev.*, 1951, **81**, 385–390.
- 57 S. J. Vosko, L. Wilk and M. Nusair, *Can. J. Phys.*, 1980, **58**, 1200–1211.
- 58 T. Van Voorhis and G. E. Scuseria, *J. Chem. Phys.*, 1998, **109**, 400–410.
- 59 F. A. Hamprecht, A. Cohen, D. J. Tozer and N. C. Handy, *J. Chem. Phys.*, 1998, **109**, 6264–6271.
- 60 A. D. Boese, N. L. Doltsinis, N. C. Handy and M. Sprik, *J. Chem. Phys.*, 2000, **112**, 1670–1678.
- 61 A. D. Boese and N. C. Handy, *J. Chem. Phys.*, 2001, **114**, 5497–5503.
- 62 A. D. Boese and N. C. Handy, *J. Chem. Phys.*, 2002, **116**, 9559.
- 63 J. M. Tao, J. P. Perdew, V. N. Staroverov and G. E. Scuseria, *Phys. Rev. Lett.*, 2003, **91**, 146401.
- 64 C. Lee, W. Yang and R. G. Parr, *Phys. Rev. B: Condens. Matter*, 1988, **37**, 785–789.
- 65 A. D. Becke, *J. Chem. Phys.*, 1993, **98**, 5648–5652.
- 66 C. Adamo and V. Barone, *J. Chem. Phys.*, 1998, **108**, 664.
- 67 M. Ernzerhof and J. P. Perdew, *J. Chem. Phys.*, 1998, **109**, 3313.
- 68 J. Heyd, G. E. Scuseria and M. Ernzerhof, *J. Chem. Phys.*, 2003, **118**, 8207.
- 69 A. J. Cohen and S. N. Handy, *Mol. Phys.*, 2001, **99**, 607.
- 70 X. Xu and W. A. Goddard III, *Proc. Natl. Acad. Sci. U. S. A.*, 2004, **101**, 2673.
- 71 A. D. Boese and L. M. L. Martin, *J. Chem. Phys.*, 2004, **121**, 3405.
- 72 A. D. Becke, *J. Chem. Phys.*, 1997, **107**, 8554.
- 73 P. J. Wilson, T. J. Bradley and D. J. Tozer, *J. Chem. Phys.*, 2001, **115**, 9233.
- 74 Y. Zhao, N. E. Schultz and D. G. Truhlar, *J. Chem. Theor. Comput.*, 2006, **2**, 364–382.
- 75 Y. Zhao and D. G. Truhlar, *Theor. Chem. Acc.*, 2008, **120**, 215–241.
- 76 Y. Zhao and D. G. Truhlar, *J. Chem. Phys.*, 2006, **125**, 194101.
- 77 A. D. Becke, *Phys. Rev. A*, 1998, **38**, 3098–3100.
- 78 J. P. Perdew, *Phys. Rev. B: Condens. Matter*, 1986, **33**, 8822–8824.
- 79 J. P. Perdew, *Phys. Rev. B: Condens. Matter*, 1986, **34**, 7406.
- 80 Y. Zhao, B. J. Lynch and D. G. Truhlar, *J. Phys. Chem. A*, 2004, **108**, 2715–2719.

- 81 J. Tao, J. P. Perdew, V. N. Staroverov and G. E. Scuseria, *Phys. Rev. Lett.*, 2003, **91**, 146401.
- 82 Y. Tawada, T. Tsuneda, S. Yanagisawa, T. Yanai and K. Hirao, *J. Chem. Phys.*, 2004, **120**, 8425.
- 83 O. A. Vydrov and G. E. Scuseria, *J. Chem. Phys.*, 2006, **125**, 234109.
- 84 O. A. Vydrov, J. Heyd, A. Kruckau and G. E. Scuseria, *J. Chem. Phys.*, 2006, **125**, 074106.
- 85 O. A. Vydrov, G. E. Scuseria and J. P. Perdew, *J. Chem. Phys.*, 2007, **126**, 154109.
- 86 T. Yanai, D. Tew and N. Handy, *Chem. Phys. Lett.*, 2004, **393**, 51.
- 87 J.-D. Chai and M. Head-Gordon, *Phys. Chem. Chem. Phys.*, 2008, **10**, 6615.
- 88 R. K. Harris, E. D. Becker, S. M. Cabral de Menezes, R. Goodfellow and P. Granger, *Pure Appl. Chem.*, 2001, **73**, 1795–1818.
- 89 M. Bühl, M. Kaupp, O. L. Malkina and V. G. Malkin, *J. Comput. Chem.*, 1999, **20**, 91–105.
- 90 D. Paschoal, B. L. Marcial, J. F. Lopes, W. B. De Almeida and H. F. Dos Santos, *J. Comput. Chem.*, 2012, **33**, 2292–2302.
- 91 F. D. Rochon and V. Buculei, *Inorg. Chim. Acta*, 2005, **358**, 2040–2056.
- 92 A. R. Khokhar, Y. Deng, S. J. Al-Baker, M. Yoshida and Z. H. Siddik, *J. Inorg. Biochem.*, 1993, **51**, 677–687.
- 93 P. Colamarino and P. L. Orioli, *J. Chem. Soc., Dalton Trans.*, 1975, 1656.
- 94 R. A. Khan, I. Guzman-Jimenez, K. H. Whitmire and A. R. Khokhar, *Polyhedron*, 2000, **19**, 975–981.
- 95 C. J. L. Lock, R. A. Speranzini and M. Zvagulis, *Acta Crystallogr., Sect. B: Struct. Crystallogr. Cryst. Chem.*, 1980, **36**, 1789.
- 96 E. G. Talman, W. Bruning, J. Reedijk, A. L. Spek and N. Veldman, *Inorg. Chem.*, 1997, **36**, 854.
- 97 J. F. Coetzee and G. R. Padmanabham, *J. Am. Chem. Soc.*, 1965, **87**, 5005–5010.
- 98 F. D. Rochon and V. Buculei, *Inorg. Chim. Acta*, 2004, **357**, 2218.
- 99 B. Beagley, B. D. W. J. Cruickshank, C. A. McAuliffe, R. G. Pritchard, A. M. Zaki, R. L. Beddoes, R. J. Cernik and O. S. Mills, *J. Mol. Struct.*, 1985, **130**, 97–102.
- 100 T. A. K. Allaf, L. J. Rashan, D. Steinborn, K. Merzweiler and C. Wagner, *Transition Met. Chem.*, 2003, **28**, 717–721.
- 101 F. D. Rochon and L. M. Gruia, *Inorg. Chim. Acta*, 2000, **306**, 193–204.
- 102 T. Kluge, M. Bette, C. Vetter, J. Schmidt and D. Steinborn, *J. Organomet. Chem.*, 2012, **715**, 93–101.
- 103 T. C. Johnstone, J. J. Wilson and S. J. Lippard, *Inorg. Chem.*, 2013, **52**, 12234–12249.
- 104 J. J. Wilson and S. J. Lippard, *Inorg. Chem.*, 2011, **50**, 3103–3115.
- 105 S. Dhar and S. J. Lippard, *Proc. Natl. Acad. Sci. U. S. A.*, 2009, **106**, 17356–17361.
- 106 A. R. Khokhar, Y. Deng, Y. Kido and Z. H. Siddik, *J. Inorg. Biochem.*, 1993, **50**, 79–87.
- 107 S. R. Ali Khan, S. Huang, S. Shamsuddin, S. Inutsuka, K. H. Whitmire, Z. H. Siddik and A. R. Khokhar, *Bioorg. Med. Chem.*, 2000, **8**, 515–521.
- 108 S. Shamsuddin, C. C. Santillan, J. L. Stark, K. H. Whitmire, Z. H. Siddik and A. R. Khokhar, *J. Inorg. Biochem.*, 1998, **71**, 29–35.
- 109 E. Petruzzella, N. Margiotta, M. Ravera and G. Natile, *Inorg. Chem.*, 2013, **52**, 2393–2403.
- 110 E. Wexselblatt, E. Yavin and D. Gibson, *Angew. Chem., Int. Ed.*, 2013, **52**, 1–5.
- 111 Y. Shi, L. Yi, S.-A. Liu, D. J. Kerwood, J. Goodisman and J. C. Dabrowiak, *J. Inorg. Biochem.*, 2012, **107**, 6–14.
- 112 E. E. Blatter, J. F. Vollano, B. S. Krishnan and J. C. Dabrowiak, *Biochemistry*, 1984, **23**, 4817–4820.
- 113 M. S. Ali, K. H. Whitmire, T. Toyomasu, Z. H. Siddik and A. R. Khokhar, *J. Inorg. Biochem.*, 1999, **77**, 231–238.
- 114 S. Neidle and C. Snoook, *Acta Crystallogr., Sect. C: Cryst. Struct. Commun.*, 1995, **51**, 822–824.
- 115 L. Chen, P. F. Lee, J. D. Ranford, J. J. Vittal and S. Y. Wong, *J. Chem. Soc., Dalton Trans.*, 1999, 1209–1212.
- 116 R. Kuroda, S. Neidle, I. M. Ismail and P. J. Sadler, *Inorg. Chem.*, 1983, **22**, 3620–3624.